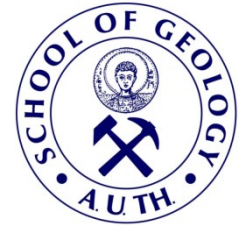




ARISTOTLE UNIVERSITY OF
THESSALONIKI
DEPARTMENT OF GEOLOGY
Laboratory of Engineering Geology and
Hydrogeology



Research Project (Code 97824)

**Groundwater depletion. Are Eco-friendly Energy Recharge
Dams a solution?**

Report of Work Package 2 / (W2/D2-3)

A graphic showing a hand holding a globe, with the word 'Groundwater Depletion' overlaid. The 'D' in 'Depletion' is green and has a leaf-like shape.

Groundwater DePLETION

PRINCIPAL INVESTIGATOR:

KAZAKIS NERANTZIS

Dr. HYDROGEOLOGIST

Funding: Hellenic Foundation for Research

& Innovation H.F.R.I.



August 2021

Table of Contents

1	Introduction	2
2	Description of the study sites.....	2
2.1	Campania region	2
2.2	Eastern Thermaikos Gulf	5
2.3	Mouriki basin	8
2.4	Marathonas basin.....	10
3	DRONE measurements.....	12
3.1	Mouriki.....	15
3.2	Vasilika.....	16
3.3	Thermi	17
3.4	K. Scholari.....	17
3.5	Lakkoma.....	18
3.6	Triadi	19
3.7	Rapentosa – Marathonas basin	20
3.8	Campania region	21
3.9	Results	21
4	Data base.....	22
4.1	GIS	22
4.2	Groundwater level measurements	23
4.3	Hydrochemical data.....	24
4.4	Meteorological data.....	24
4.5	Soil moisture and temperature.....	25
4.6	Thematic Maps	26
5	Data network.....	26
5.1	Groundwater level measurements	26
5.2	Groundwater quality measurements.....	28
5.3	Dam water quality	30
5.4	Meteorological data.....	31
5.5	Vadose zone measurements – Geoelectrical measurements	33
6	1 st Article in scientific journal	36
7	Conclusions	37
8	References	38

1 Introduction

The report of work package 2 includes the description of all areas under study, the description of the data base and network (deliverables D2-1 and D2-2), the drone results, the analysis (diagrams) of the data from meteorological stations and the 1st publication of the project including the analysis of meteorological data and initial simulation.

2 Description of the study sites

The description of the four areas under study is presented in this section. Three sites are located in Greece, while one site is located in Italy.

2.1 Campania region

The Upper Volturno and Calore basin is located in the Campania region (on the Tyrrhenian side of the Southern Apennines, Italy). The study area is about 5.613 km², while the altitude varies from 16 m to 2118 m. The mean annual temperature is 16.4 °C and the mean annual rainfall is 1245 mm. The geological setting of the Upper Volturno-Calore basin consists of dolomites, limestones, sandstones, clay-marl flysch, and pyroclastic fall deposits (**Figure 2.1**).

The main aquifer is hosted in alluvial formations with a mean thickness of 60 m. The elevation varies from 15.5 m and 2.102 m (**Figure 2.2**). Agricultural and livestock activities are mainly located in the lowlands, whereas mixed forests and pastures constitute the land cover of the mountainous part. The main crop types are vineyards, cereals, vegetables, and orchards (**Figure 2.2**).

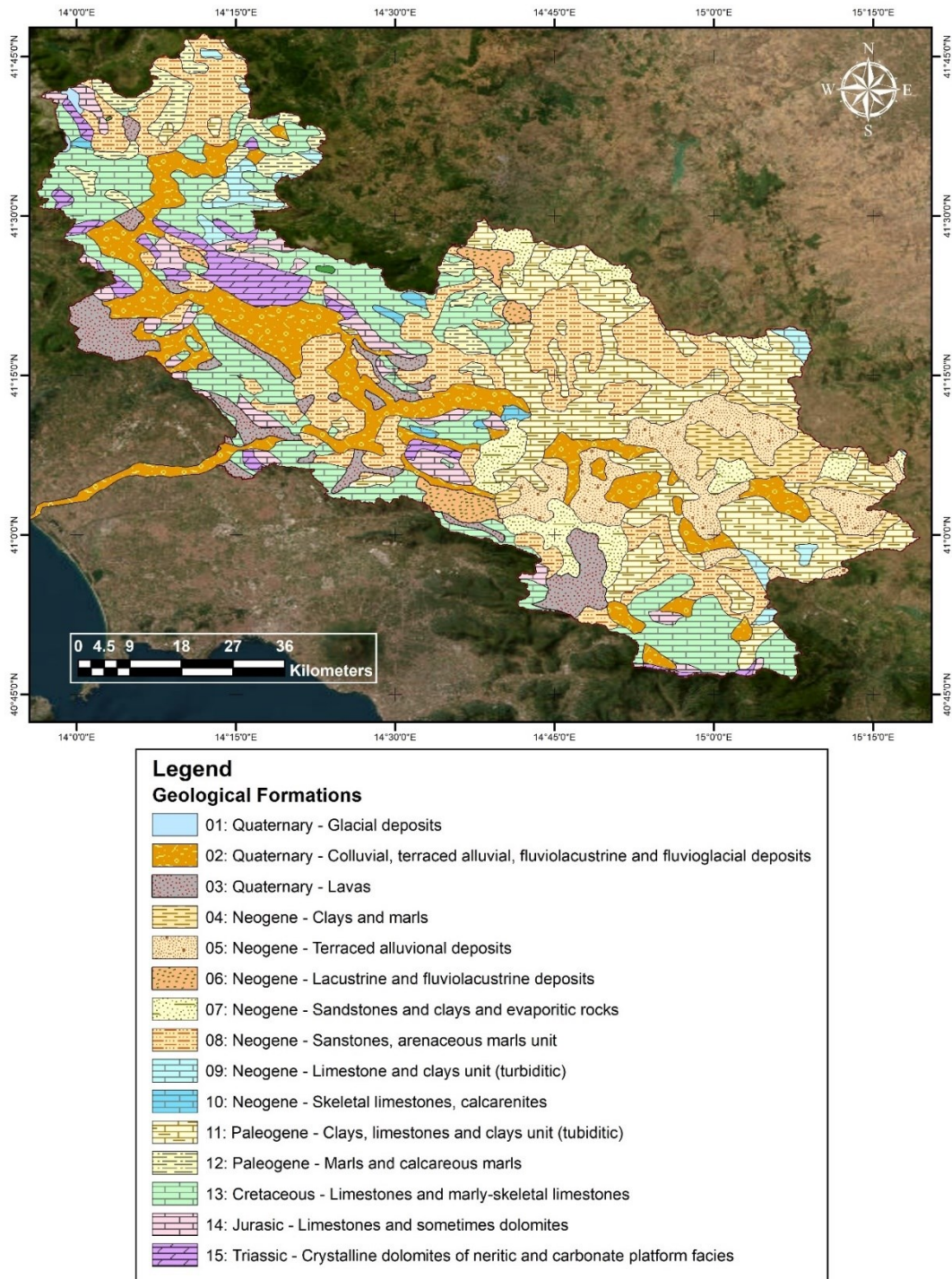


Figure 2.1 Geological map for Upper Volturno-Calore basin.

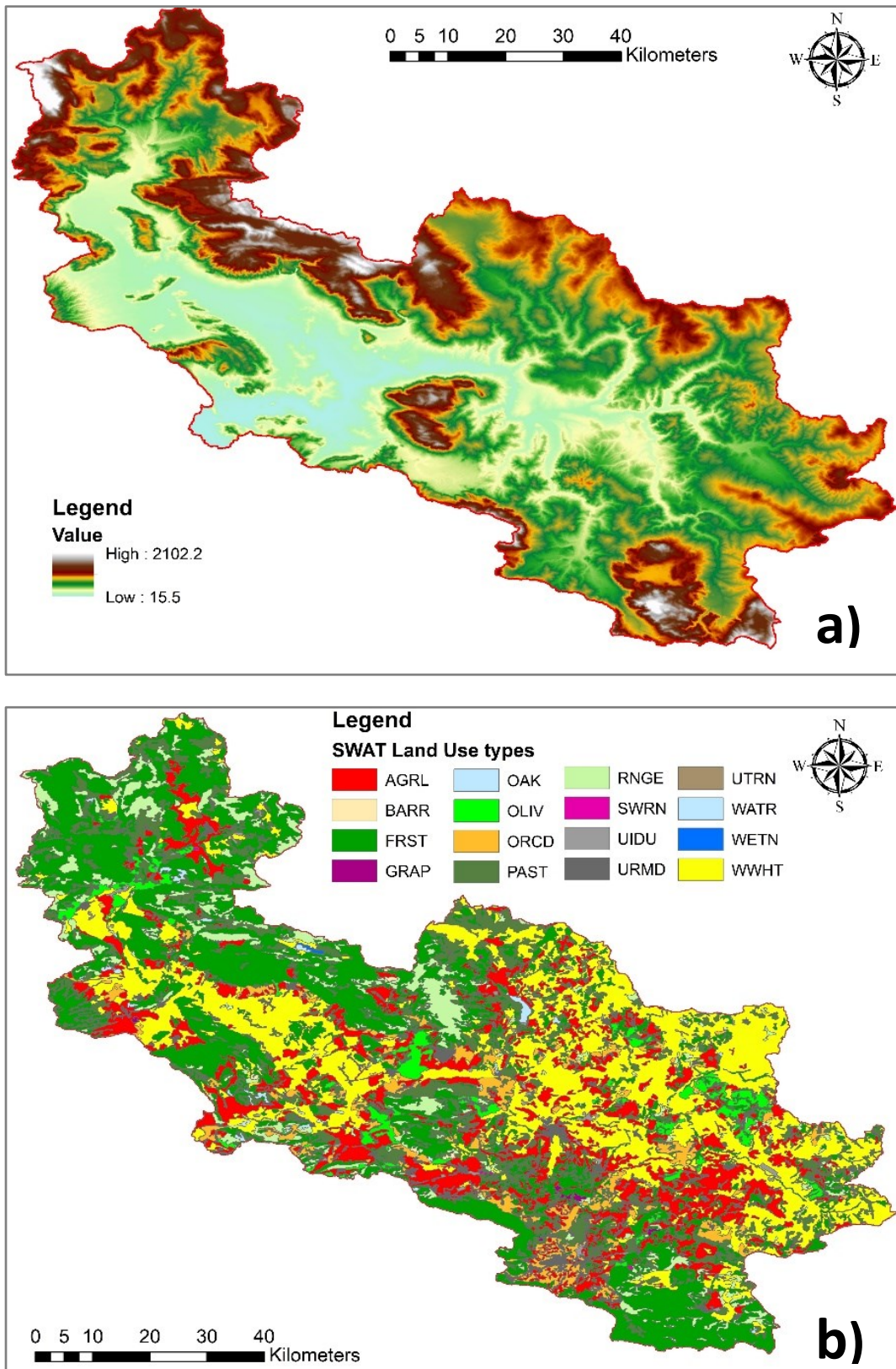


Figure 2.2 Spatial distribution of elevation (a), and land use dominance (b) in Upper Volturno-Calore basin.

2.2 Eastern Thermaikos Gulf

Eastern Thermaikos Gulf is located in northern Greece. The basin covers an area of 932.7 km², with altitudes ranging from 0 m (coastal zone) to 1199 m a.s.l (Mount Hortiatis) (Figure 2.3). The climate is a typical Mediterranean semi-arid climate with dry summers and wet winters. The mean annual temperature and precipitation values are 15.1°C and 575 mm, respectively.

The geological setting of Anthemountas basin is presented in **Figure 2.4**. The basin is characterized by a multiple aquifer system consisting of various aquifer types: i) a porous aquifer hosted in the Quaternary and Neogene sediments, ii) a karst aquifer located in the south-central part of the basin, and iii) fractured rock aquifers in the mountainous part of the basin.

Agriculture is the primary economic activity of the area, although tourism has increased in recent years, mainly during the summer. The area's main crops include vegetables, olives, wine grapes, corn and cereals (**Figure 2.5**). The area's growing domestic and irrigation water requirements are met by numerous boreholes located in the porous aquifers. Due to overexploitation, groundwater depletion has been observed in the aquifer.

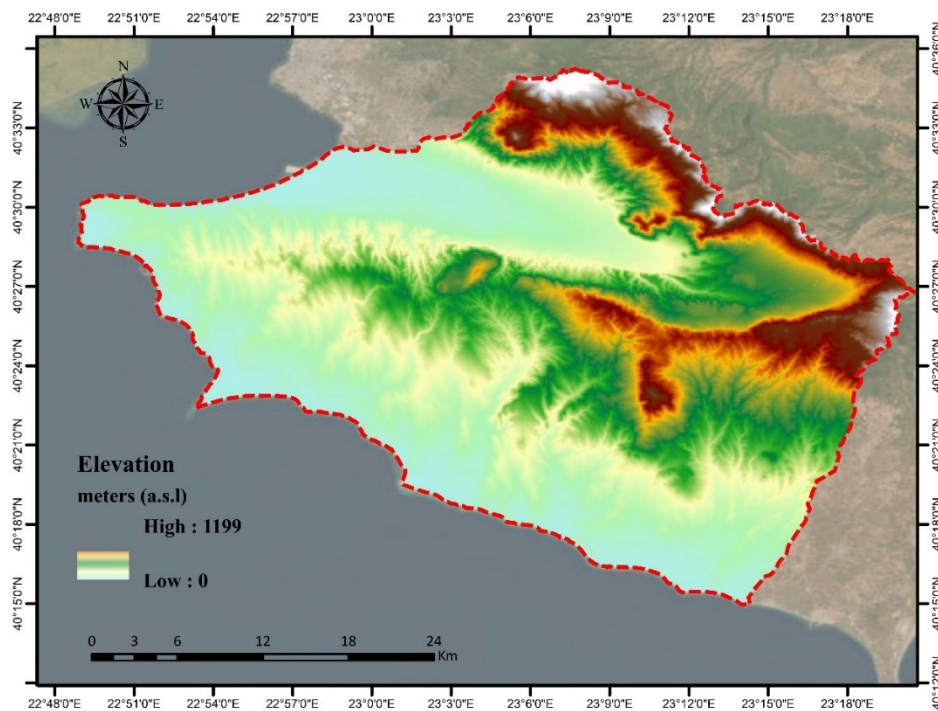
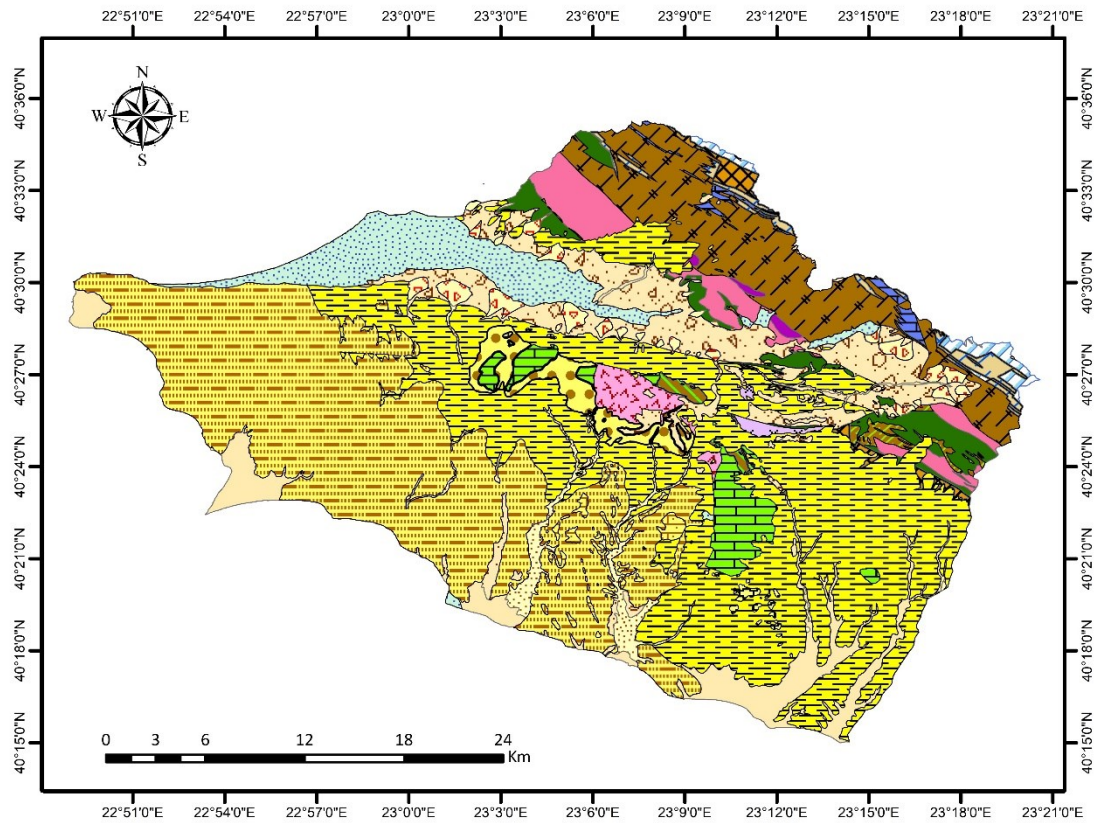


Figure 2.3 Spatial distribution of elevation in Eastern Thermaikos Gulf.



Legend

Geology


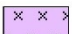
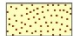


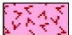


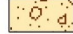



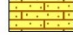



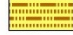







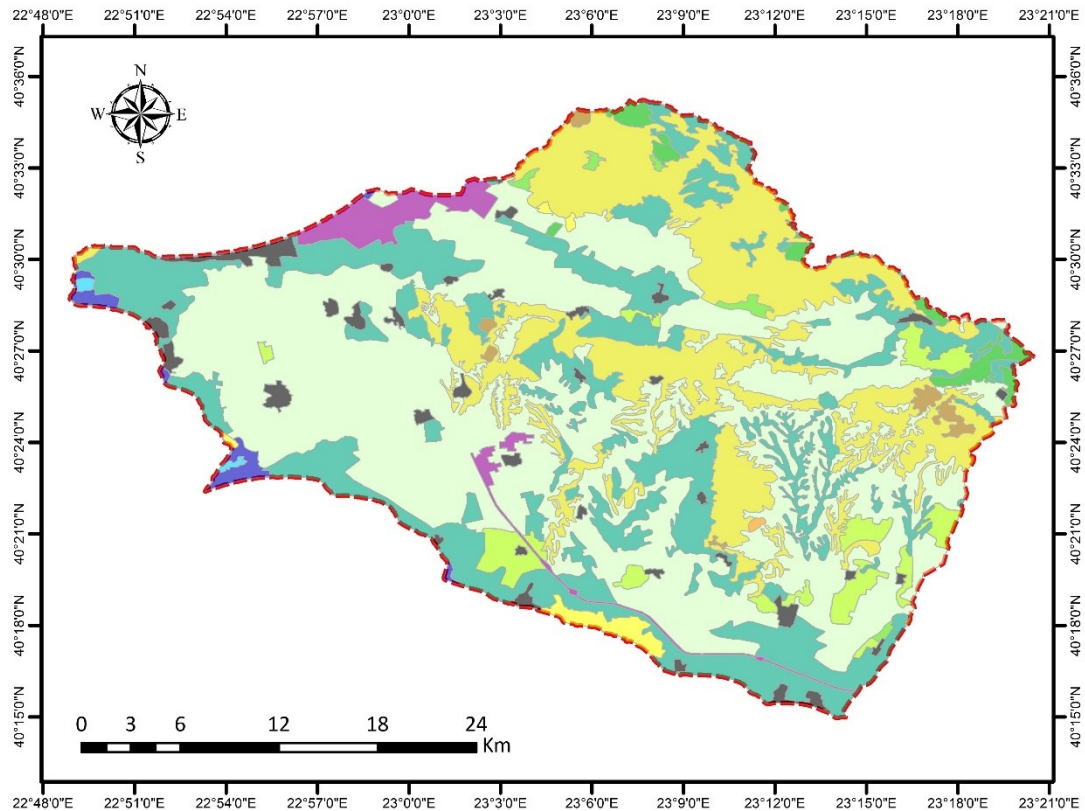
	Holocene: Alluvial deposits		Mesozoic: Epidote - actinolite schist
	Holocene: Lower stage of lowest terrace system		Mesozoic: Gabbro
	Holocene: Valley deposits		Mesozoic: Granodiorite
	Pleistocene: Fans		Mesozoic: Limestones
	Pleistocene: Terrace systems		Mesozoic: Phyllites (Svoula group)
	Neogene: Basic conglomerate series		Mesozoic: Pyroxenites
	Neogene: Fresh water Limestones		Mesozoic: Quartzites (Svoula group)
	Neogene: Red clay series		Mesozoic: Shales
	Neogene: Sandstone - marl series		Mesozoic: Ultramafic rocks
	Neogene: Travertine limestones		Mesozoic: Leucocratic gneiss
	Mesozoic: Clay-Schists		Mesozoic: Limestones recrystallized
	Mesozoic: Diorite (complex of Yerakini)		Paleozoic: Two-mica gneiss (Vertiskos formation)

Figure 2.4 Geological map for Eastern Thermaikos Gulf.



Legend

LandUse

Artificial surfaces

- Urban fabric
- Industrial, commercial and transport units
- Mine and construction sites
- Artificial, non-agricultural vegetated sites

Agricultural areas

- Arable land
- Permanent crops
- Pastures
- Heterogenous agricultural areas

Forests and semi natural areas

- Forests
- Scrub and heraceous vegetation associations
- Open spaces with little or no vegetation

Wetlands and water bodies

- Inland wetlands
- Maritime wetlands
- Inland waters
- Marine waters

Figure 2.5 Spatial distribution of land use dominance in Eastern Thermaikos Gulf.

2.3 Mouriki basin

The Mouriki basin is located in the north part of Kozani Prefecture in northern central Greece (Figure 1). It is an inland basin with a surface area of 110 km². The climate is semi-arid Mediterranean with moderate rainfall during summer. The average annual air temperature and precipitation values are 11.2°C and 636 mm, respectively. The geological setting of the study area is presented in **Figure 2.6**.

The main aquifer system is hosted in alluvial deposits with a mean thickness of 70 m covering an area of 30.5 km². The groundwater flow follows the local morphology moving towards the lowlands in an SSW to NNE direction. The mean altitude of the study area is 874.5 m a.s.l. with a mean slope inclination of 26.1% (**Figure 2.7**). Livestock and agriculture are the main activities in the area and the main cultivations are corn, cereal crops, fruit trees, vegetables and legumes. The mountainous part of the basin is covered with mixed, coniferous forest vegetation (**Figure 2.7**).

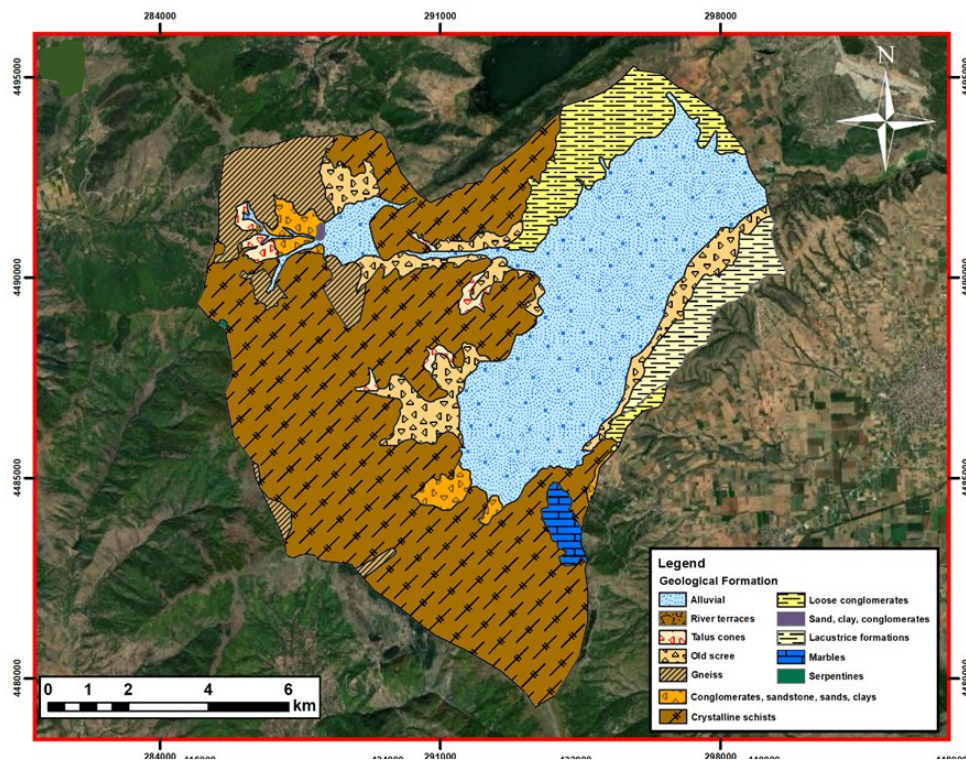


Figure 2.6 Geological map for Mouriki basin.

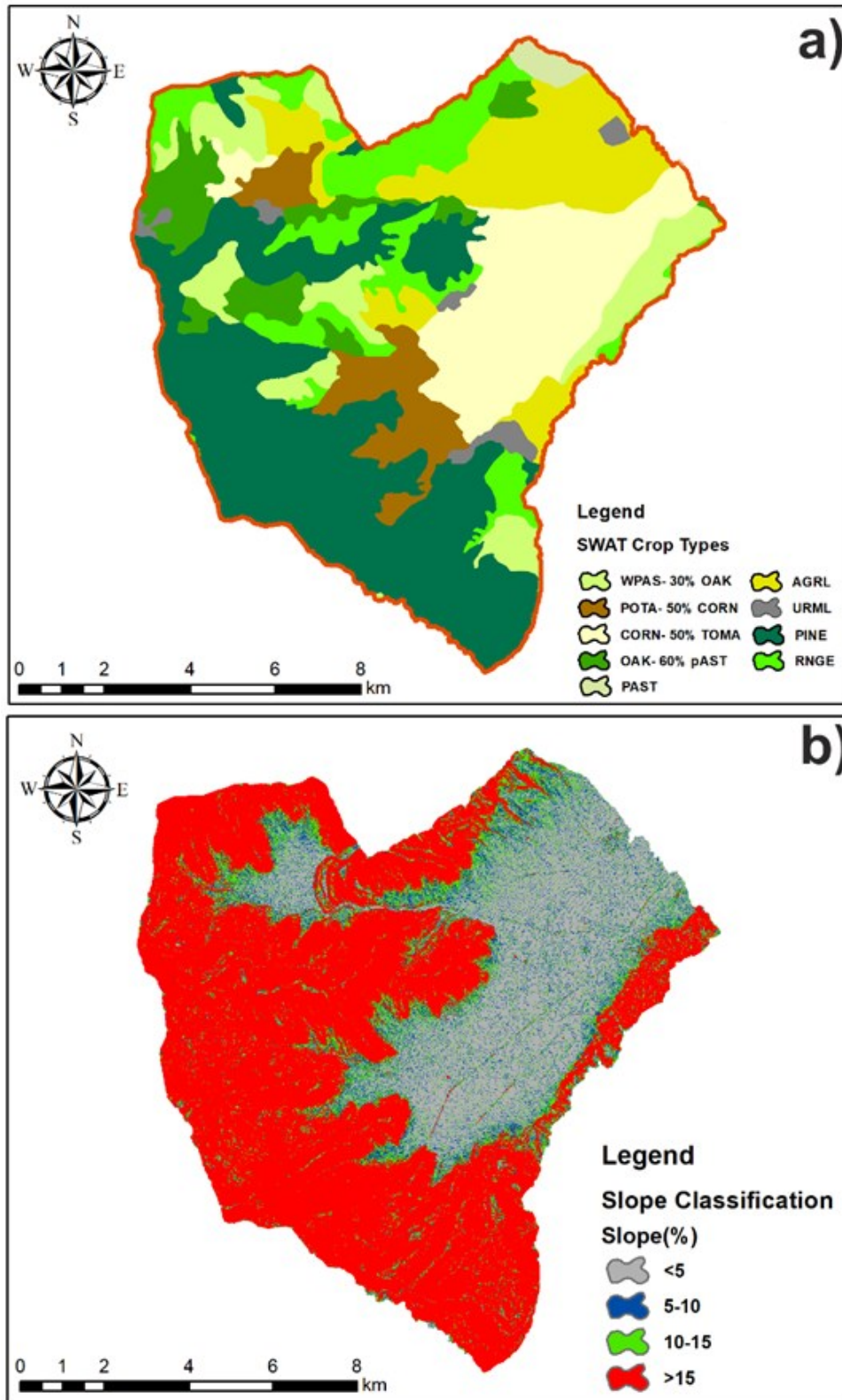


Figure 2.7 Spatial distribution of land use dominance (a) and slope classes (b) in Mouriki basin.

2.4 Marathonas basin

The plain of Marathonas is located in the eastern part of Attica, southern Greece. The basin covers an area of 182.6 km². The elevation ranges from 0 m to 1407 m and is characterized as flat with gentle slopes in the central part and semi-mountainous to mountainous in the limits with the mountainous mass of Parnitha (**Figure 2.8**). The area is characterized by numerous environmental protection zones such as the national park of Parnitha and the mountain range of Penteli which are extended around the basin of Marathon. The average annual air temperature and precipitation values for the period 2011-2020 are 15.7 °C and 477.4 mm, respectively. The study area is classified in the Attic-Cycladic zone of the Aegean. The geological formations are divided into alluvial deposits, marbles-limestones, schists, and serpentines. Intensive erosion phenomena and small-scale soil movements are presented in the area due to the erosive nature of the formations. A porous aquifer is in the coastal area of the site, whereas karstic aquifers are found in areas underlain by marbles.

The main part of the region is covered by urban areas, forests (pine, mixed forest, sclerophyllous vegetation), shrubs, oak, pasture, cultivated fields, and wetlands (**Figure 2.9**) with spatial and temporal variations in their extent during the last years while devastating fire destroyed a notable part of the vegetation in 2009. Groundwater is mainly used for domestic use and irrigation in the sub-urban coastal zone. Both aquifers are subjected to intense pumping due to extensive agricultural activities, with an extended irrigation period (greenhouses) in most of the plain.

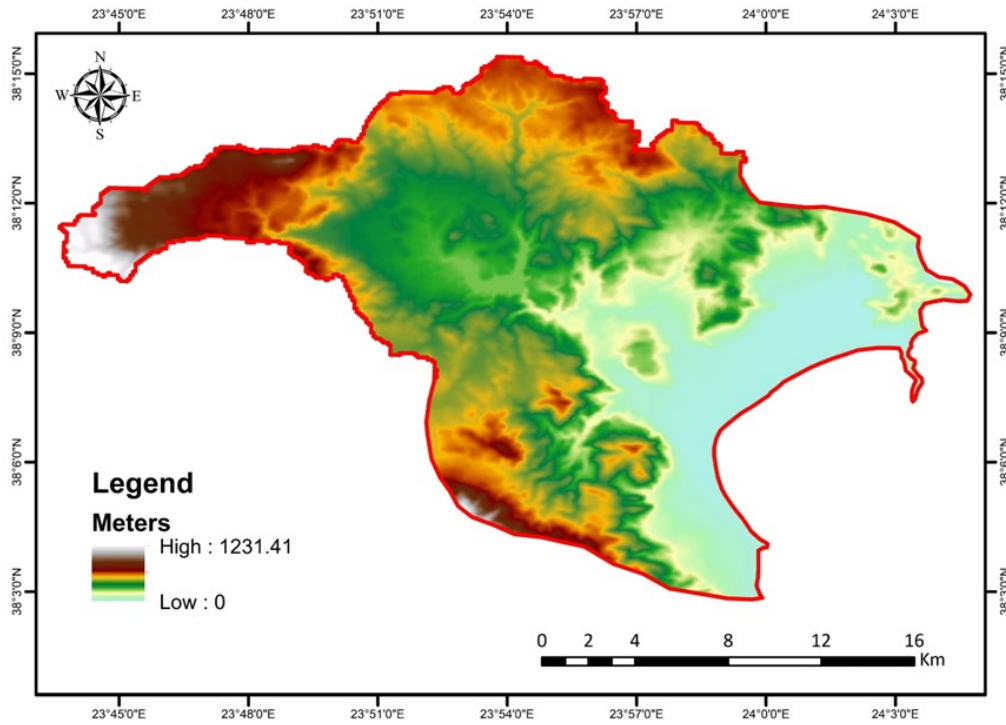


Figure 2.8 Spatial distribution of elevation in Marathonas basin.

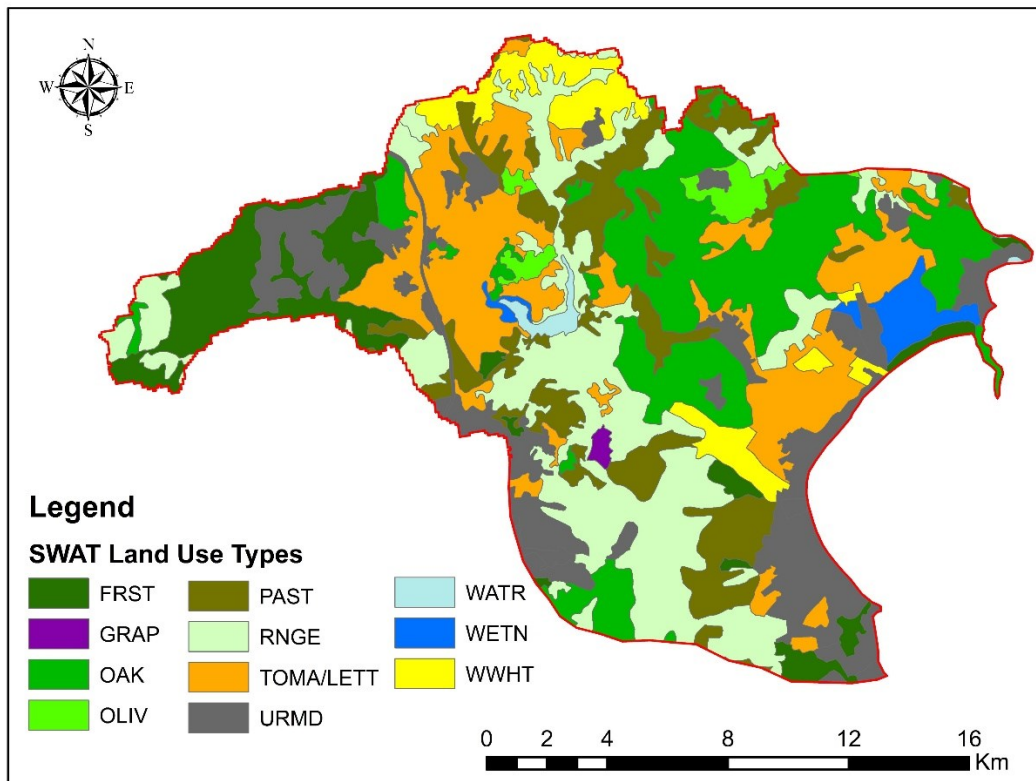


Figure 2.9 Spatial distribution of land use dominance in Marathonas basin.

3 DRONE measurements

A more technical, widely used term is UAV (Unmanned Aerial Vehicle). Equally often the term UAS (Unmanned Aircraft System) is used. The terms RPA (Remotely Piloted Aircraft) and RPAS (Remotely Piloted Air System) are also in use. The common reference point of all these terms is, of course, the unmanned aircraft. Flying such an aircraft can be either predestined, when there is practically no operator, or remotely piloted in real time. Remote piloting is made possible via the control station and the navigational software. The general legal context of Unmanned Aircraft Systems (UAS) of Greece is defined mainly in two sheets of Government Gazette (FEK 3152/B/30-9-2016 & FEK B-4527/30.12.2016).

The official definition given for the Unmanned Aircraft System - UAS, is the following: “Unmanned Aircraft System” – UAS is defined as the unmanned aircraft (UA) with all the relevant equipment concerning its support (control station, data connection and remote piloting capabilities, navigational equipment etc.), which is necessary for operating the unmanned aircraft. The UAS are either free or they can be tethered on a stable or moving base. The category of unmanned aircraft systems – UAS also includes remotely - piloted aircrafts – RPA and remotely piloted aircraft Systems - RPAS, as well as the autonomous aircrafts”.

UAS are suitable for topographical tasks, due to the products they offer. Lightweight digital cameras, as well as great focal length cameras, can be placed on UAS. Topographical maps, photomosaics, 3D digital surface models and 3D point clouds, of high accuracy, can be produced, with the proper processing of the images. Their application mainly refers to small and medium-sized areas to also satisfy the financial factor. Prior to each flight a flight plan needs to be submitted in DAGR.

During field work and after the needed acquaintance with the study area has been achieved, the flight plan can follow. Here, a few factors intervene, affecting each other. For example, the flight duration might be limited. Therefore, its orbit should be accordingly adjusted so that the optimal use of time is achieved. Afterwards, other elements, must be decided, such as the flight altitude, the photo overlap, the resolution and the shooting angle. The use or not of photostats depends on the

capacity of the equipment. Therefore, if, for example, the navigation system used can provide a satisfactory accuracy of the shooting point coordinates, placing photostats is not necessary. Therefore, if this is not possible, prior to the flight, the appropriate points should be researched and marked. This means that their distribution in the area of interest should be isomeric and moreover, visible and recognizable from the captured photos. For each such point, its coordinates should be defined with the highest accuracy possible (e.g., by using a geodetic station or RTK GNSS).

Prior to liftoff it is considered good, by examining the flight plan, to locate some convenient points for an emergency, manual landing. From then on, since the radio connection quality has been checked and the communication between the aircraft and the transmitter has been confirmed, lift off can start as well as data downloading. During the process, there should be a quality check of the data, through the control station, so that it can be repeated in case of an error and if considered necessary. In this study the double-frame, flight pattern is used for better results, which is suitable for producing a detailed three-dimensional model of the surveyed area. They are two frame patterns, vertically intertwined with each other, for optimal performance. This pattern gives the capability of a partly oblique photo-surveying, as well as the studied objects displaying from all four orientations. This way, the study area and the objects comprising the latter can be displayed from different angles.

To sum up, the individual processes materialized by the SfM software are:

- automatic orientation of the images by locating homologous characteristic features in all the images through an identification of their descriptors,
- solving the aerial-triangulation, excluding rough errors in measurements and simultaneous self-calibration,
- automatic collection of the area point cloud through a multi-image, algorithm identification (local/global matching),
- eliminating the noise and creating a digital elevation model (of the surface or the ground),
- creating a real orthophotography/orthophotomosaic by automatically checking concealed points and combining textures from multiple images,

- creating a fully three-dimensional object model (three-dimensional triangulation) with real photo-texture.

These procedures, even though they can be performed almost without human intervention, they do not ensure, in the majority of the cases, satisfactory results, especially in those cases where the demand in resolution and accuracy is high, as is the case in topographic surveying. In such applications, a sophisticated handling is required, so that the errors are located and properly corrected. Thus, frequently enough, an exclusion of specific areas or even whole images is required, single-image but also stereoscopic correction of counterparts during orientation, enforcement of the geometry and points distribution, introduction of three-dimensional edges as discontinuity lines in order to limit inconsistencies in the points cloud, sophisticated algorithms of three-dimensional triangulation and modelling with a simultaneous application of up-to-date noise-reduction algorithms and subservice during the orthophotomosaic production phase.

There are multiple types of UAS polycopters/drones (**Figure 3.1**), while for each type a different type of UAS operator license (**Figure 3.2**). In the case of the GrecoDam report, the use of UAS was deemed as crucial in the mapping of the various dams and their surrounding areas, with the data captured being used in the Pix4D program. For the needs of the present study, automated flights were executed, using a DJI Phantom pro V2 UAS and the Pix4Dcapture software, in order to capture georeferenced, framed orthophotographs.



Figure 3.1 Different drones / polycopters.

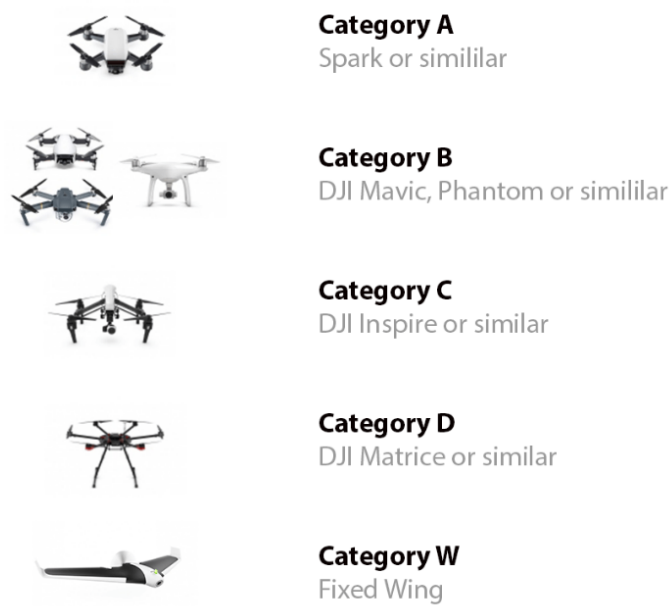


Figure 3.2 UAV - UAS types.

3.1 Mouriki

The Mouriki dam is located in the Prefecture of Western Macedonia, in the Municipality of Mouriki, west of the city of Ptolemaida. It's a Gravity – type dam, built to cover the irrigational needs of the local region during the summer period. It has a crest of 321 meters long, its base is 114 meters wide, and has a height of 20 meters, while it covers an area of 0,043 km² with a perimeter of 0,91 km (Figure 3.3, Figure 3.4).

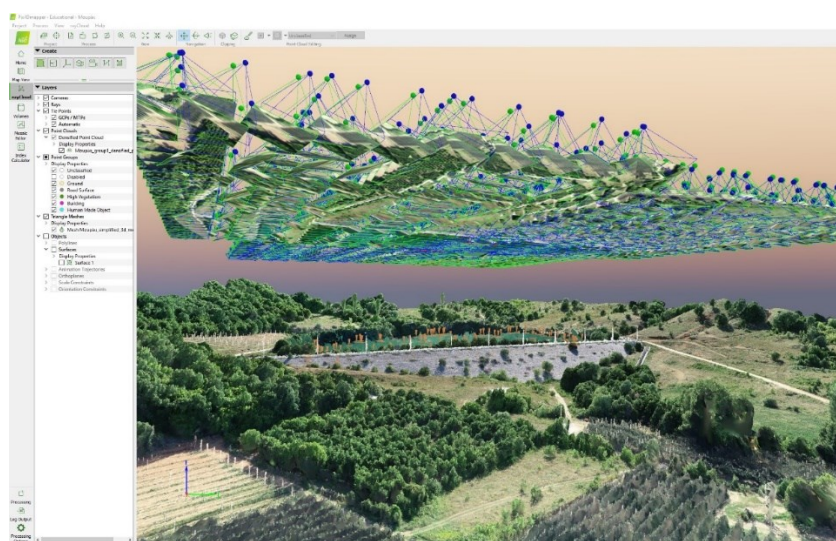


Figure 3.3 Image still from the Pix4D orthophoto processing program.

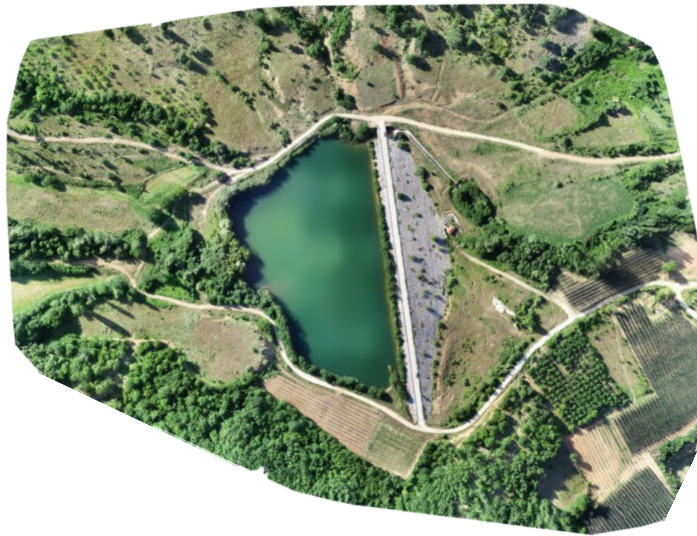


Figure 3.4 Orthomosaic of Mouriki dam.

3.2 Vasilika

The Vasilika dam is located in the Prefecture of Central Macedonia, in the Municipality of Vasilika, north of the city of Vasilika. It's a Gravity – type dam, built to cover the irrigational needs of the local region during the summer period. It has a crest of 177 meters long, its base is 120 meters wide, and has a height of 20 meters, while it covers an area of 0,038 km² with a perimeter of 1,13 km (**Figure 3.5**).

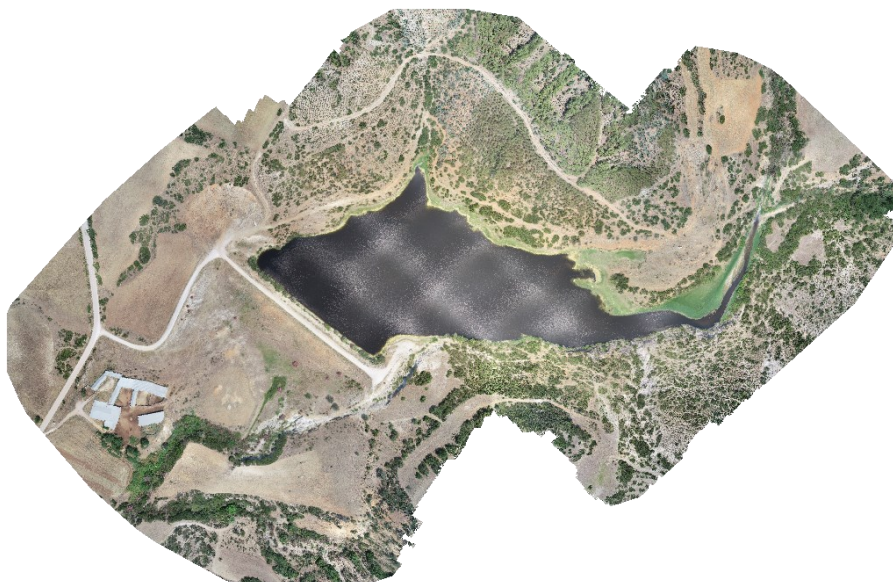


Figure 3.5 Orthomosaic of Vasilika. Dam.

3.3 Thermi

The Thermi dam is located in the Prefecture of Central Macedonia, in the Municipality of Thermi, north - east of the city of Thermi. It's a Gravity – type dam, built to cover the irrigational needs of the local region during the summer period, as well as serve as a park for the local population. It has a crest of 71 meters long, its base is 67 meters wide, and has a height of 11 meters, while it covers an area of 0,041 km² with a perimeter of 1,36 km (Figure 3.6).



Figure 3.6 Orthomosaic of Thermi dam.

3.4 K. Scholari

The Kato Scholari dam is located in the Prefecture of Central Macedonia, in the Municipality of Nea Propontida, south of the village of Kato Scholari. It's a Gravity – type dam, built to cover the irrigational needs of the local region during the summer period. It has a crest of 128 meters long, its base is 85 meters wide, and has a height

of 11 meters, while it covers an area of 0,041 km² with a perimeter of 1,36 km (Figure 3.7).



Figure 3.7 Orthomosaic of K. Scholari.

3.5 Lakkoma

The Lakoma dam is located in the Prefecture of Central Macedonia, in the Municipality of Nea Propontida, east of the village of Kato Scholari. It's a Gravity – type dam, built to cover the irrigational needs of the local region during the summer period. It has a crest of 125 meters long, its base is 75 meters wide, and has a height of 10 meters, while it covers an area of 0,028 km² with a perimeter of 1,34 km (Figure 3.8).



Figure 3.8: Orthomosaic of Lakkoma dam.

3.6 Triadi

The Triadi dam is located in the Prefecture of Central Macedonia, in the Municipality of Themi, north - east of the city of Triadi. It's a Gravity – type dam, built to cover the irrigational needs of the local region during the summer period, as well as serve as a park for the local population. It has a crest of 145 meters long, its base is 67 meters wide, and has a height of 145 meters, while it covers an area of 0,045 km² with a perimeter of 1,22 km (**Figure 3.9**).



Figure 3.9 Orthomosaic of the Triadi dam.

3.7 Rapentosa – Marathonas basin

The dam height is 15 m, 28 m long gravity dam with a crest width of 145 m and base width of 28 m. The dam elevation is 223 m above sea level while the dam crest is at 145 m. The reservoir has a maximum depth of 54 m and surface area of 0.03 km² (**Figure 3.10**).



Figure 3.10 Orthomosaic of Rapentosa dam.

3.8 Campania region

In the Campania region we could achieve to obtain DRONE measurements of the Dam, however the critical data obtained from the literature and the analysis of satellite images. It has a crest of 147 meters long, its base is 110 meters wide, and has a height of 10 meters, while it covers an area of 1 km² (Figure 3.11).



Figure 3.11 Satellite image of the dam in Campania plain.

3.9 Results

According to the above methodology, the technical characteristics of the dams are shown in Table 3.1. This result will be used for the modeling and optimization of dam operation.

Table 3.1 Technical characteristics of the dams

A/A	Dam	Height (m)	Crest (m)	Width	Area (km ²)	Type
1	Mouriki	20	321	114	0,043	Gravity
2	Vasilika	20	177	120	0,038	Gravity
3	Thermi	11	71	67	0,041	Gravity
4	K. Scholari	11	128	85	0,041	Gravity
5	Lakkoma	10	125	75	0,028	Gravity
6	Triadi	12	145	67	0,045	Gravity
7	Rapentosa	15	145	28	0,03	Gravity
8	Campania	10	147	110	1	Gravity

4 Data base

In the framework of the project, we established a data base structure which includes a common folder in Dropbox with name GREcoDAM. Additionally, individual folders have been established between the members of the research group for data sharing in Onedrive and Dropbox (**Figure 4.1**). Within the shared folder are included all the climatological data in commonly used formats as excel files, figures and maps, corel files and geospatial data in GIS environment. The size of the data per file ranges from a few KB to a few hundreds of MB.



Figure 4.1 Shared folder platforms used for GREcoDAM data base sharing.

4.1 GIS

The GIS data base uses the ArcCatalog as the main tool for the data elaboration (**Figure 4.2**). The structure includes the following folders with the file types respectively:

- Raster: A raster image is an image file format that's defined by a pixel with one or more numbers associated with it. The number defines the location, size, or colour of the pixels. The raster files are DEM, Slope, Precipitation, Water quality data, Hydraulic data etc.
- Polygons: A polygon is one of three feature types with which almost all spatial data is depicted in GIS. Polygons are invariably depicted as vector data, as opposed to raster data. Polygons include geology, Corine land cover, Cities, Crops etc.
- Polylines: A polyline is one of three feature types with which almost all spatial data is depicted in GIS. Polylines are invariably depicted as vector data, as opposed to raster data. Polylines include roads, drainage network, faults etc.
- Points: A point is one of three feature types with which almost all spatial data is depicted in GIS. Points are invariably depicted as vector data, as opposed to raster data.

«Groundwater depletion. Are Eco-friendly Energy Recharge Dams a solution?»

- Maps: Include all produced thematic maps in jpg and tiff format. Includes all Geological, Morphological, Hydrogeological, Vulnerability and all thematic maps.

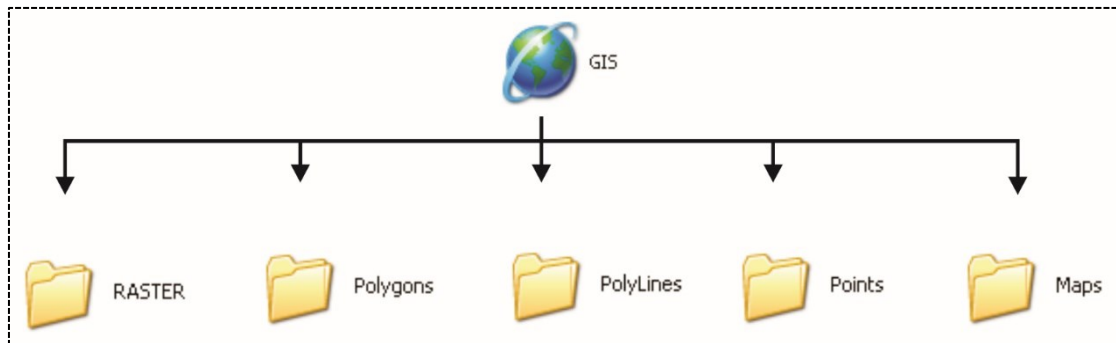


Figure 4.2 Data base structure in GIS environment.

4.2 Groundwater level measurements

Groundwater level measurements constitute a critical parameter for the implementation of the project. More specifically, groundwater depth variation will be used for models' validation and conceptualization of the hydrogeological regime. All measurements are included in excel files in the dropbox common folder (Figure 4.3). Additionally in the data base are included diagrams of groundwater fluctuation coupled with other parameters. An example is presented in Figure 4.4.

The screenshot shows an Excel spreadsheet for well CM18. The columns represent dates from 2008 to 2022, grouped by month. The rows represent various parameters. The first few rows are highlighted in green and yellow. The main data area has a repeating pattern of pink and light blue cells. The last few rows are highlighted in red and yellow.

	2008	5-6/2/2021	26-27/2/2021	3-4/4/2021	4-6/5/2021	20/05/2021	20/06/2021	03/07/2021	30-31/07/2021	31/08/2021	31/09/2021	30-31/10/2021	18/11/2021	10/02/2022																	
Μήκος	73.6	64.44	28.3	45.3	27.06	46.54	26.93	48.61	25.45	48.35	29.2	47.4	27.3	46.5	28.07	45.53	28.97	44.63	29.01	44.55	29.69	43.93	27.07	45.63	27.43	46.37	26.8	48.8	27.2		
Πλάτος	11.2	-7.26	14.44	-3.24	13.85	-2.83	14.44	-3.26	14.5	-3.3	16.57	-5.37	14.5	-3.3	21.87	-10.67	22.85	-11.65	21.5	-10.3	18.82	-7.62	17.07	-5.87	15.38	-4.38	14.44	-3.24	14.8		
Υψόμετρο	38.2	38.2	38.7	4.31	31.27	4.31	31.28	8.7	31.1	5.2	32.5	7	31.2	6.74	31.46	7.25	30.95	7	30.5	8.41	29.72	8.38	29.22	7.88	30.22	7.55	30.45	8.55	31.65	9.4	
Εμβαδόν	82.6	85.1	53.64	31.31	53.09	31.01	54.05	30.88	54.24	29.44	55.66	31.05	54.06	31.02	54.06	28.25	56.65	31.68	51.42	31.72	53.16	52.36	52.74	52.43	51.27	52.28	52.81	52.06	53.04	53.11	
Εμβαδόν	44	288.8	270.23	17.3	270.5	17.87	270.55	17.83	270.57	16.78	272.02	18.12	270.68	17.92	270.88	18.27	270.55	21.74	267.06	18.63	269.97	19.21	269.55	18.27	270.55	18.19	270.61	17.68	271.12	18.44	
Εμβαδόν	46	274.9	220.27	23.91	250.99	20.66	19.74	255.35	21.5	253.44	20.66	21.5	253.44	20.66	20.66	21.86	253.04	20.9	234	19.13	255.77	21.86	253.04	20.9	234	19.13	255.77	21.86	253.04	20.9	
Εμβαδόν	52	283	249.1	16.89	246.52	16.58	246.42	16.54	246.46	16.53	247.2	17.31	245.89	16.53	246.41	17.32	245.88	16.09	244.93	16.21	244.61	16.85	244.15	17.09	245.03	17.03	245.61	16.27	246.73	14.6	
Εμβαδόν	205	32.8	-8.41	21.1	-4.3	20.87	-4.03	20.72	-7.61	16.54	-3.14	20.7	-7.8	10.74	-7.61	20.9	-4	21.25	-4.25	11.93	-4.21	10.89	-4.09	10.61	-4.01	10.81	-4.01	10.7	20.7		
Εμβαδόν	184	20.4	-15.4	33.86	-13.26	33.83	-13.23	34.03	-13.67	34.5	-14.1	34.51	-14.11	34.49	-14.09	36.57	-16.17	37.1	-16.7	37.3	-17.1	36.07	-15.87	35.1	-14.7	34.42	-14.02	33.62	-13.22	34.03	
Εμβαδόν	180	61.3	-15.2	78.35	-13.45	79.93	-14.63	78.74	-13.48	79.7	-14.4	80.46	-13.16	78.93	-13.61	83.31	-16.01	85.12	-13.82	84.32	-13.02	81.14	-15.84	80.09	-14.79	84.01	-16.71	83.4	-18.1	80.4	
Εμβαδόν	125	28.5	-21.9	76	-17.5	74.8	-16.2	74	-15.5	58.68	-13.8	60.3	-13.6																		
Εμβαδόν	25.5	-8.41	30.62	-1.12	30.81	-0.81	30.46	-0.96	31.52	-2.02	30.7	-1.2	30.77	-1.27	31.76	-2.26	31.4	-1.9	31.13	-1.65	30.92	-1.42	30.67	-1.17	30.49	-0.99	30.75	-1.25	30.6		
Εμβαδόν	25.2	6.4	28.49	-3.29	28.5	-3.3	28.5	-3.3	29	-3.8	29	-3.8	28.84	-3.84	31.13	-5.93	31	-5.8	30.63	-5.43	29.48	-4.28	29.2	-4	28.74	-3.54	28.36	-3.16	28.31		
Εμβαδόν	102.8	8.0	33.39	9.62	33.1	9.7	33.03	9.77	33.1	9.7	33.2	9.6	33.21	9.59	33.83	9.17	34.25	8.51	34.63	8.17	34.2	8.51	34.63	8.17	34.2	8.51	34.63	8.17	34.2	8.51	
Εμβαδόν	68.4	-4.91	73.1	-4.7	72.36	-4.94	72.33	-4.73	73.1	-4.8	74.69	-4.29	72.35	-4.95	74.93	-4.19															

Figure 4.3 Excel file with groundwater measurements.

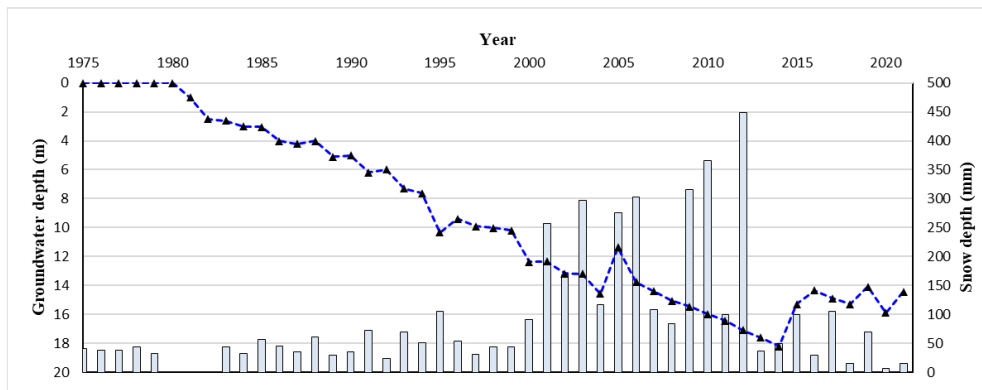


Figure 4.4 Diagram of groundwater depth variation coupled with snow depth.

4.3 Hydrochemical data

The quality of groundwater and dam water constitute another critical parameter for the determination of the pollution regime of the study sites. All data from the chemical analysis are included in excel files in the dropbox common folder (Figure 4.5).

Sample	pH	EC (µS/cm)	hardness	CO ₃ (mg/L)	CO ₃ (mg/L)	Cl (mg/L)	SO ₄ (mg/L)	NO ₂ (mg/L)	NO ₃ (mg/L)	PO ₄ (mg/L)	F (mg/L)	Na (mg/L)	K (mg/L)
GD1	7.7	849	33.3	397	ND	61.4	16.8	ND	21.2	0.13	ND	48.1	1.94
GD2	8	954	44.4	458	ND	56	73	0.017	10.7	0.2	ND	45	1.34
GD3	7.5	1487	27.14	477	ND	76	53	0.56	34.1	0.13	ND	245	1.88
GD4	8	861	49	567	ND	8.7	4.8	ND	23.2	0.08	ND	7.4	0.94
GD5	7.9	574	27	329	ND	15	23	ND	ND	0.03	ND	21.3	0.6
GD6	7.4	639	22.2	281	ND	36	40	ND	17	0.09	ND	52	4.1
GD7	8.2	592	26.9	323	ND	23	11	ND	12.3	0.03	ND	23	1.5
GD8	7.2	1938	61.9	817	ND	247	40	ND	5	0.12	ND	202	7
GD9	7.1	1339	54	665	ND	127	32	0.015	13	1.04	ND	103	7.9
GD10	7.5	1914	63.1	470	ND	320	54.1	ND	72	0.05	ND	148.1	2.4
GD11	7.5	1443	48.5	525	ND	157	32	ND	91.8	0.04	ND	125	2.5
GD12	6.9	1536	60.5	793	ND	115	36	ND	2	0.15	ND	111	5.4
GD13	7.1	1652	67.3	796	ND	156	32	ND	13	0.07	ND	105	13
GD14	7.2	1556	48.8	726	ND	135	88	ND	ND	0.14	ND	175	4.7
GD15	7.6	1050	36.7	390	ND	105	46	ND	21	ND	ND	75	3.5
GD16	7.5	833	32.445	378	ND	66	25	ND	11	ND	ND	67	2.7
GD17	7.4	10522	252.6	372	ND	3195	546	ND	212	0.08	ND	1365	46.8

Figure 4.5 A table from excel with chemical data.

4.4 Meteorological data

The data base includes meteorological data from the study sites. The meteorological data includes rainfall, snowfall, temperature, wind, solar radiation etc. These data are obtained from open access online databases (e.g. <https://www.meteo.gr/>) as well as from a meteorological station that established in the framework of the project in the Anthemountas basin. Additionally, the data from four stations that handled from the research group are used for implementation of the project (Stations: Kozani, Simonos Petra A, B and C), while the location of the stations are formed in kmz and shapefiles. The data are saved in csv, txt and excel

files within the dropbox folder (Figure 4.6), while within the excel files are included also graphs of the meteorological data (Figure 4.7).

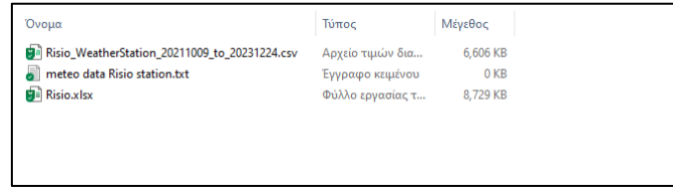


Figure 4.6 Example of meteorological data files.

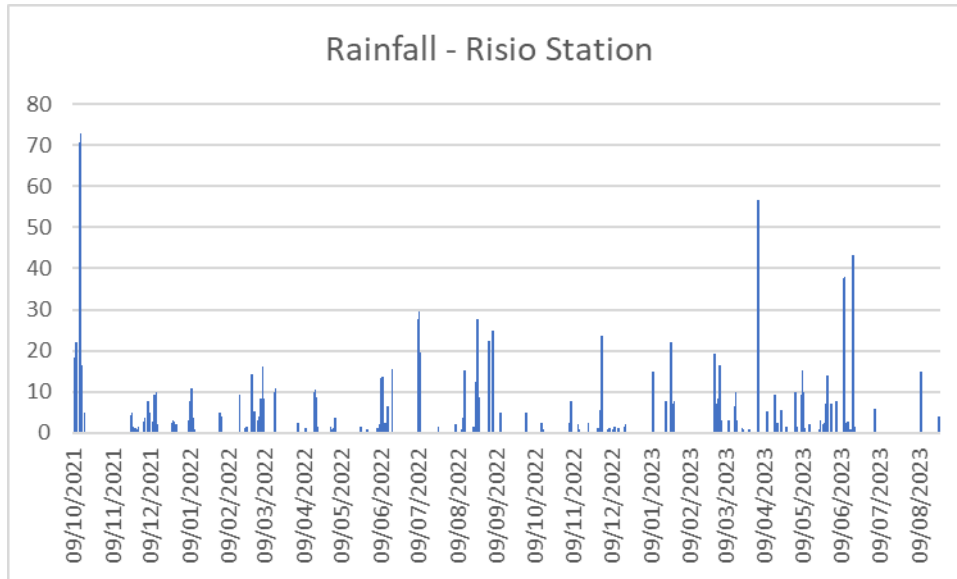


Figure 4.7 Representative graph of the Risio Station.

4.5 Soil moisture and temperature

Within Anthemountas basin, we establish an instrument for soil moisture and temperature monitoring up to 1 m. Similar to the other data, the soil moisture and temperature is shared within the dropbox folder in excel files (Figure 4.8).

Date	Temperature [°C] at -0.05 [m]	Temperature [°C] at -0.15 [m]	Temperature [°C] at -0.25 [m]	Temperature [°C] at -0.35 [m]	Temperature [°C] at -0.45 [m]	Temperature [°C] at -0.55 [m]	Temperature [°C] at -0.65 [m]	Temperature [°C] at -0.75 [m]	Temperature [°C] at -0.85 [m]	Soil water content [mm] at
29/09/2021 04:11	19.77	22.51	23.74	23.54	23.25	22.87	23.13	22.98	22.95	22.95
29/09/2021 04:12	19.77	22.51	23.74	23.54	23.25	22.87	23.13	22.98	22.95	22.95
29/09/2021 04:13	19.77	22.51	23.74	23.54	23.33	22.82	23.21	22.98	22.95	22.95
29/09/2021 04:14	19.77	22.51	23.74	23.54	23.2	22.87	23.13	22.98	22.95	22.95
29/09/2021 04:15	19.77	22.51	23.74	23.54	23.31	22.92	23.13	22.98	22.95	22.95
29/09/2021 04:16	19.77	22.51	23.74	23.54	23.25	22.84	23.13	22.98	22.95	22.95
29/09/2021 04:17	19.77	22.51	23.74	23.54	23.31	22.82	23.21	22.98	22.95	22.95
29/09/2021 04:18	19.77	22.51	23.74	23.54	23.28	22.84	23.21	22.98	22.95	22.95
29/09/2021 04:19	19.74	22.51	23.74	23.54	23.2	22.82	23.16	22.98	22.95	22.95
29/09/2021 04:20	19.77	22.51	23.74	23.54	23.28	22.82	23.18	22.98	22.95	22.95
29/09/2021 04:21	19.74	22.51	23.74	23.54	23.25	22.92	23.15	22.98	22.95	22.95
29/09/2021 04:22	19.72	22.51	23.74	23.54	23.28	22.89	23.19	22.98	22.95	22.95
29/09/2021 04:23	19.77	22.51	23.74	23.54	23.25	22.92	23.15	22.98	22.95	22.95
29/09/2021 04:24	19.77	22.51	23.74	23.54	23.2	22.89	23.16	22.98	22.95	22.95
29/09/2021 04:25	19.74	22.48	23.74	23.54	23.2	22.84	23.18	22.98	22.95	22.95
29/09/2021 04:26	19.77	22.51	23.74	23.54	23.23	22.89	23.13	22.98	22.95	22.95
29/09/2021 04:27	19.77	22.48	23.74	23.54	23.2	22.87	23.15	22.98	22.95	22.95
29/09/2021 04:28	19.77	22.48	23.74	23.54	23.28	22.89	23.18	22.98	22.95	22.95
29/09/2021 04:29	19.77	22.51	23.74	23.54	23.28	22.89	23.18	22.98	22.95	22.95
29/09/2021 04:30	19.68	22.51	23.74	23.54	23.23	22.92	23.16	22.98	22.95	22.95
29/09/2021 04:31	19.74	22.45	23.74	23.54	23.31	22.89	23.19	22.98	22.95	22.95
29/09/2021 04:32	19.69	22.38	23.74	23.54	23.23	22.79	23.18	22.98	22.95	22.95
29/09/2021 04:33	19.72	22.51	23.74	23.54	23.25	22.87	23.18	22.98	22.95	22.95
29/09/2021 04:34	19.74	22.43	23.74	23.54	23.2	22.84	23.13	22.98	22.95	22.95
29/09/2021 04:35	19.64	22.35	23.74	23.54	23.25	22.97	23.13	22.98	22.95	22.95
29/09/2021 04:36	19.57	22.38	23.74	23.54	23.23	22.89	23.13	22.98	22.95	22.95
29/09/2021 04:37	19.72	22.38	23.71	23.54	23.25	22.92	23.16	22.98	22.95	22.95
29/09/2021 04:38	19.72	22.35	23.74	23.54	23.18	22.92	23.16	22.98	22.95	22.95
29/09/2021 04:39	19.64	22.38	23.74	23.54	23.23	22.87	23.23	22.98	22.95	22.95
29/09/2021 04:40	19.72	22.33	23.74	23.54	23.31	22.89	23.19	22.98	22.95	22.95
29/09/2021 04:41	19.59	22.43	23.71	23.54	23.28	22.84	23.19	22.98	22.95	22.95
29/09/2021 04:42	19.69	22.38	23.74	23.54	23.23	22.84	23.13	22.98	22.95	22.95
29/09/2021 04:43	19.67	22.31	23.74	23.54	23.28	22.89	23.13	22.98	22.95	22.95
29/09/2021 04:44	19.59	22.3	23.74	23.54	23.33	22.89	23.19	22.98	22.95	22.95
29/09/2021 04:45	19.57	22.27	23.71	23.54	23.28	22.89	23.21	22.98	22.95	22.95
29/09/2021 04:46	19.59	22.3	23.74	23.54	23.28	22.87	23.15	22.98	22.95	22.95
29/09/2021 04:47	19.69	22.3	23.74	23.54	23.28	22.87	23.18	22.98	22.95	22.95
29/09/2021 04:48	19.67	22.3	23.71	23.54	23.25	22.87	23.15	22.98	22.95	22.95
29/09/2021 04:49	19.57	22.33	23.71	23.54	23.28	22.92	23.21	22.98	22.95	22.95
29/09/2021 04:50	19.67	22.3	23.74	23.54	23.28	22.94	23.16	22.98	22.95	22.95
29/09/2021 04:51	19.67	22.3	23.74	23.54	23.2	22.87	23.15	22.98	22.95	22.95
29/09/2021 04:52	19.67	22.33	23.74	23.54	23.25	22.89	23.15	22.98	22.95	22.95
29/09/2021 04:53	19.59	22.3	23.74	23.54	23.25	22.84	23.13	22.98	22.95	22.95

Figure 4.8 Soil moisture and temperature data in excel files.

4.6 Thematic Maps

The data base includes also the output of the data elaboration. For each study area there is a folder (Figure 4.9) including several thematic maps such as geological, morphological and groundwater quality maps (Figure 4.10).

Όνομα	Τύπος	Μέγεθος	Τίτλος
MAPS Anthemountas	Φάκελος αρχείων		
MAPS mouriki	Φάκελος αρχείων		
MAPS marathonas	Φάκελος αρχείων		
MAPS campania	Φάκελος αρχείων		

Figure 4.9 Folders of the thematic maps.

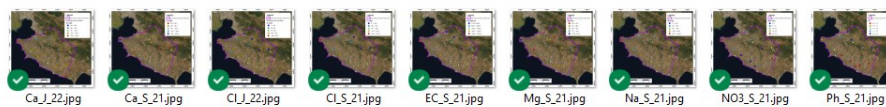


Figure 4.10 Thematic maps of the data base.

5 Data network

The implementation of the project requires various data which will be collected from field measurements, laboratory analysis and data bases. For the implementation of the project the following data will be collected:

- Groundwater level,
- Groundwater quality,
- Dam water quality,
- Resistivity measurements of the vadose zone
- Meteorological data,

All data will be stored in the shared folder within Dropbox in the corresponding files (e.g. excel, txt, shape files). The sampling collection and analysis will follow the Standard Methods for the Examination of Water and Wastewater (Rice et al., 1999) and the "National field manual for the collection of water-quality data" (USGS 2015).

5.1 Groundwater level measurements

Groundwater level measurements were planned for two periods (Dry and Wet periods). In the framework of the project water level measurement was obtained for two periods in the Marathonas and Campania sites (September 2021 – May 2022). In

Mouriki basin we measured for two hydrological years during wet and dry periods (September 2021 – May 2022 – September 2022 – May 2023). In Anthemountas basin we measured for two hydrological years during wet and dry periods (September 2021 – May 2022 – September 2022 – May 2023) as well as for the dry period of September 2023. Additionally, in Anthemountas we obtained monthly measurements from the period of September 2021 until September 2023. The detailed measurements in Anthemountas basin were decided after the initial results of the project which showed that the depletion problem occurs mainly in Anthemountas basin.

The number of the measurement points for each site is described below:

Anthemountas basin: The groundwater level measurements obtained in 95 boreholes for the periods September 2021 – May 2022 – September 2022 – May 2023 – September 2023. The monthly measurements were obtained in 35 boreholes for the period between September 2021 to September 2023 (**Figure 5.1**).

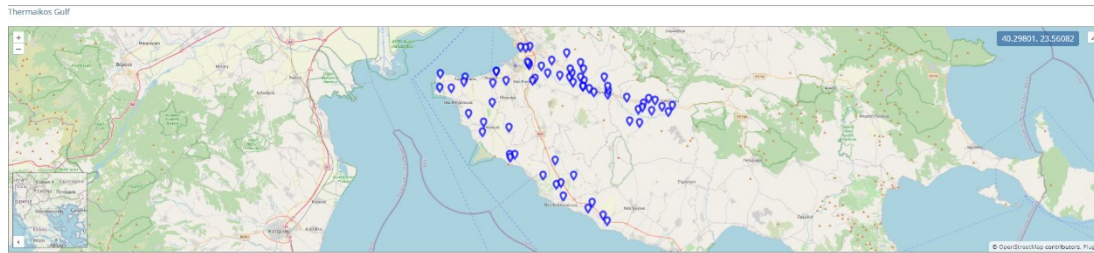


Figure 5.1 Locations of groundwater level measurements in the Eastern Thermaikos – Anthemountas basin.

Mouriki basin: The groundwater level measurements obtained in 30 boreholes for the periods September 2021 – May 2022 – September 2022 – May 2023 (**Figure 5.2**).

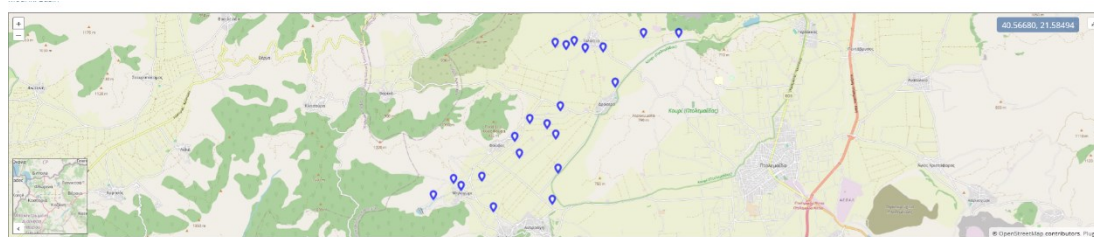


Figure 5.2 Locations of groundwater level measurements in the Mouriki basin.

Marathonas basin: The groundwater level measurements obtained in 21 boreholes for the periods September 2021 – May 2022. The locations are shown in the map of Figure 5.3.

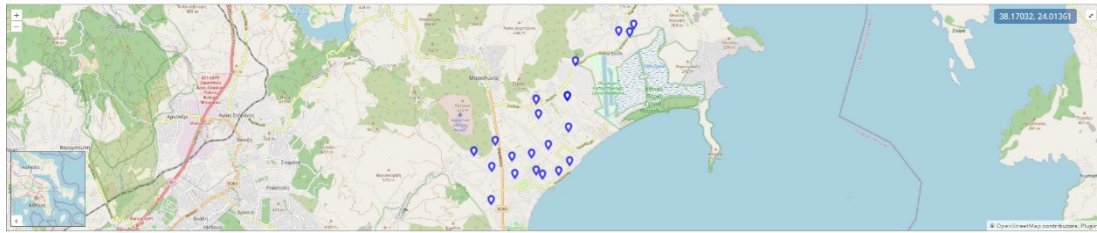


Figure 5.3 Locations of groundwater level measurements in the Marathonas basin.

Campania plain: The groundwater level measurements obtained in 15 boreholes for the periods September 2021 – May 2022 (**Figure 5.4**).

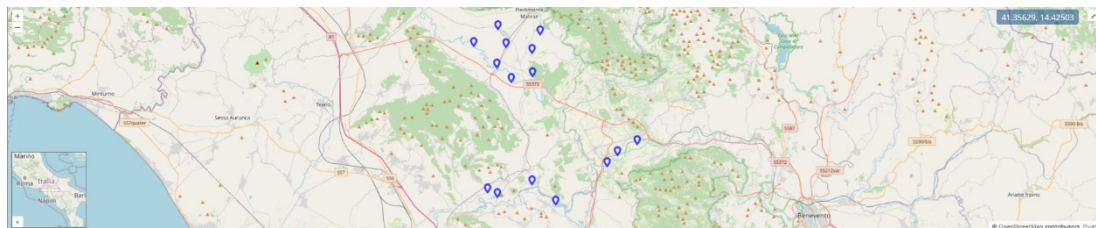


Figure 5.4 Locations of groundwater level measurements in the Campania site.

All data were included in shape files for the creation of thematic maps and txt files as inputs for the simulation models. The locations of the measurement points are also presented on the website of the project (<https://groundwater-ecodams.web.auth.gr/>).

5.2 Groundwater quality measurements

Groundwater water samples were collected from all sites for two periods (Dry and Wet periods). According to the initial plan the chemical analysis includes the following parameters: HCO_3 , CO_3 , Cl , SO_4 , NO_2 , NO_3 , PO_4 , Na , K , Ca , Mg , Li , Sr , NH_4 , As and Cr . However, we measured more elements in all sites. The analysis of the Greek sites obtained in Aristotle University of Thessaloniki, while the samples from the Italian site obtained in the University of Campania. The chemical analysis for the Greek sites includes the following parameters: pH , EC , Eh , T , Total hardness, HCO_3 , CO_3 , Cl , SO_4 , NO_2 , NO_3 , PO_4 , F , Na , K , Ca , Mg , Li , Sr , NH_4 , Sb , Se , As , Cd , Cr (VI), Cr , Cu , Fe , Pb , Mn , Ni , Co , Mo , Zn , Hg , SiO_2 , B , T.O.C . In the Italina site, the chemical analysis includes the following parameters: T , pH , EC , Eh , HCO_3 , NH_4 , F , NO_3 , SO_4 , Na , K , Cl , Mg , Ca , Li , B , Al , V , Mn , Fe , Ni , Cu , Zn , Cr , As , Rb , Sr , Ba , U .

Additionally in selected samples obtained analysis of ^3H , ^2H and ^{18}O . The number of the measurement points for each site is described below:

Anthemountas basin: In total seventeen (17) samples were collected from boreholes for the Dry and Wet periods of September 2021 and May 2022 (**Figure 5.5**). Additionally monthly measurements of pH, EC, Eh, T obtained in a Karst Spring of the site. Moreover, obtained multi-layer measurements of T and EC in two boreholes.

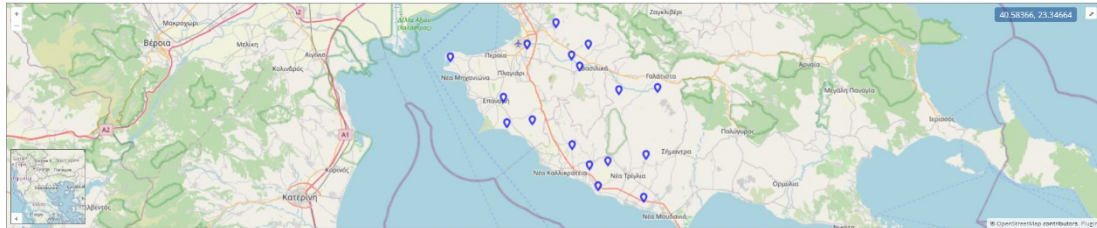


Figure 5.5 Locations of groundwater samples in the Eastern Thermaikos – Anthemountas basin.

Marathonas basin: In Marathonas basin collected ten (10) samples from boreholes for the Dry and Wet period of September 2021 and May 2022. The location of water sampling collection is shown in **Figure 5.6**.

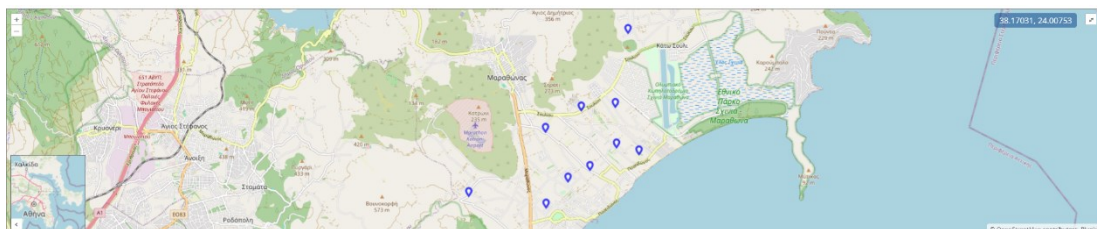


Figure 5.6 Locations of groundwater samples in the Marathonas basin.

Mouriki basin: In Mouriki basin collected eight (8) samples from boreholes for the Dry and Wet periods of September 2021 and May 2022. The locations are shown in **Figure 5.7**.

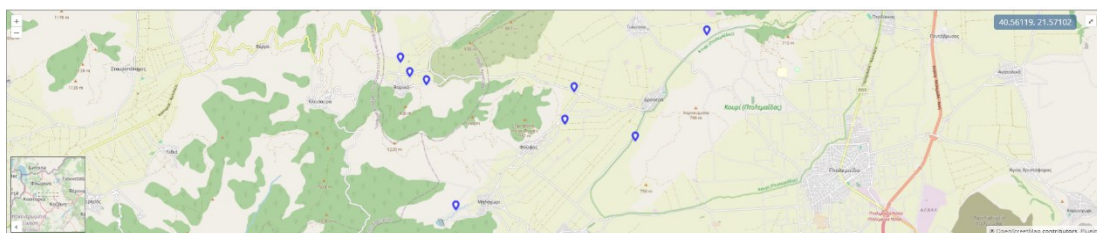


Figure 5.7 Locations of groundwater samples in the Mouriki basin.

Campania plain: In Campania plain collected in total twenty-two (22) samples from boreholes for the Dry period, while for the Wet period were collected 7 samples (There was no access to all sampling points) (**Figure 5.8**).

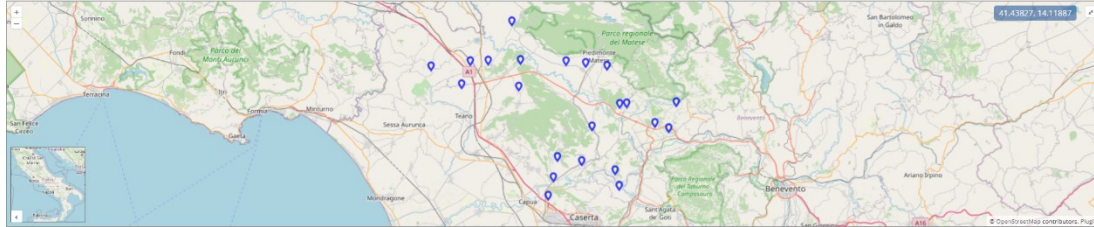


Figure 5.8 Locations of groundwater samples in the Campania basin.

The locations of the measurement points are presented on the website of the project (<https://groundwater-ecodams.web.auth.gr/>), while in the corresponding thematic maps will be presented in the scientific publications and the next deliverables of the project.

5.3 Dam water quality

For the determination of dam water quality collected samples from the eight (8) dams for the Dry period of September 2021 and Wet period of May 2022. According to the initial plan the chemical analysis includes the following parameters: HCO_3 , CO_3 , Cl, SO_4 , NO_2 , NO_3 , PO_4 , Na, K, Ca, Mg, Li, Sr, NH_4 , As and Cr. However, we measured more elements in all sites. The analysis of the Greek sites was obtained in the Aristotle University of Thessaloniki, while the samples from the Italian site were obtained in the University of Campania. The chemical analysis for the Greek sites includes the following parameters: pH, EC, Eh, T, Total hardness, HCO_3 , CO_3 , Cl, SO_4 , NO_2 , NO_3 , PO_4 , F, Na, K, Ca, Mg, Li, Sr, NH_4 , Sb, Se, As, Cd, Cr(VI), Cr, Cu, Fe, Pb, Mn, Ni, Co, Mo, Zn, Hg, SiO_2 , B, T.O.C. In the Italian site the chemical analysis includes the following parameters: T, pH, EC, Eh, HCO_3 , NH_4 , F, NO_3 , SO_4 , Na, K, Cl, Mg, Ca, Li, B, Al, V, Mn, Fe, Ni, Cu, Zn, Cr, As, Rb, Sr, Ba, U.

The locations of the measurement points are shown in **Figure 5.9**, while the locations are also presented on the website of the project (<https://groundwater-ecodams.web.auth.gr/>).

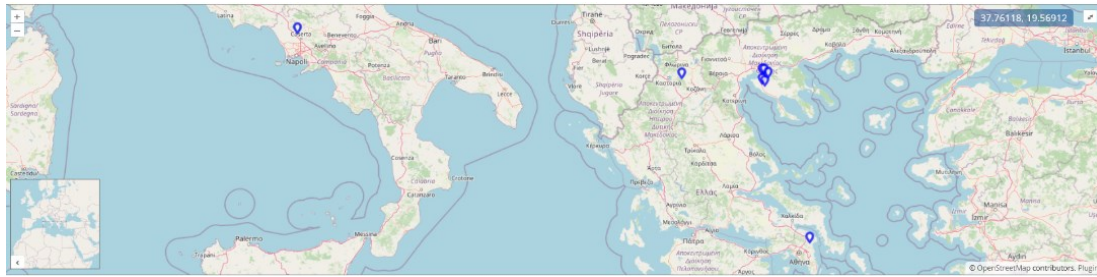


Figure 5.9 Location of the studied Dams.

5.4 Meteorological data

For the implementation of the project were used meteorological data (**Figure 5.10**) from the following sources:

- **Zoodochos Pigi station** (handled by AUTH – Coordinator Prof. Kazakis Nerantzis). Data used: Snowfall, Precipitation, Temperature, Evapotranspiration (calculated with Penman–Monteith method). The data was collected with hourly step. The data are available from February 2019 – December 2022.
- **Mount Athos 3 stations** (handled by AUTH – Coordinator Prof. Kazakis Nerantzis). Data used: Snowfall, Precipitation, Temperature, Evapotranspiration (calculated with Penman–Monteith method). The data was collected with hourly step. The data are available from February 2021 – December 2022.
- **Risio station** (handled from AUTH – Coordinator Prof. Kazakis Nerantzis) Data used: Precipitation, Temperature. The data was collected with a 10-minute step. The data are available from October 2021 – December 2023.
- **Campania region** nine (9) stations (handled by Italian Authorities). The stations are the Alife, Bagnoli Irpino, Benevento, Sorgenti Grassano, Trevico, Colle Sannita, Forli del Sannio, Isernia, and Fornelli. Data used: Precipitation, Temperature. The data are available in daily step. The data are available from January 2002 – December 2014.

[\(http://193.206.192.214/servletsdailyutm/serietemporalidaily400.php/](http://193.206.192.214/servletsdailyutm/serietemporalidaily400.php/)

[https://centrofunzionale.regione.campania.it/#/pages/sensori/sensor-utility\)](https://centrofunzionale.regione.campania.it/#/pages/sensori/sensor-utility)

- **Marathonas basin** one (1) station named Dionysos Attiki (<http://dionysos-penteli.meteoclub.gr/>). Data used: Precipitation, Temperature. The data are available in daily step. The data used was from January 2011 – December 2020. Three more stations named Marathonas, Rafina, and Schinas (handled from EMY) have been found near to the study area but contain large data gaps and couldn't be used.
- **Mouriki basin** has two (2) stations named Kozani (<http://www.meteo.gr>) and Aristotelis (<http://www.windfinder.com>). Data used: Precipitation, Temperature. The data are available from January 2017 to December 2021 for Kozani station and from January 2000 to December 2013 for Aristotelis station. The data are available in daily step.
- **Makedonia Airport** station (Handled by EMY). Data used: Precipitation, Temperature. The data used was from January 1996 – December 2020. The data are available in daily step.
- MODIS datasets were used for data collection for all sites for the parameters that were used such as snowfall, evapotranspiration, precipitation, and temperature (<https://appears.earthdatacloud.nasa.gov/>).

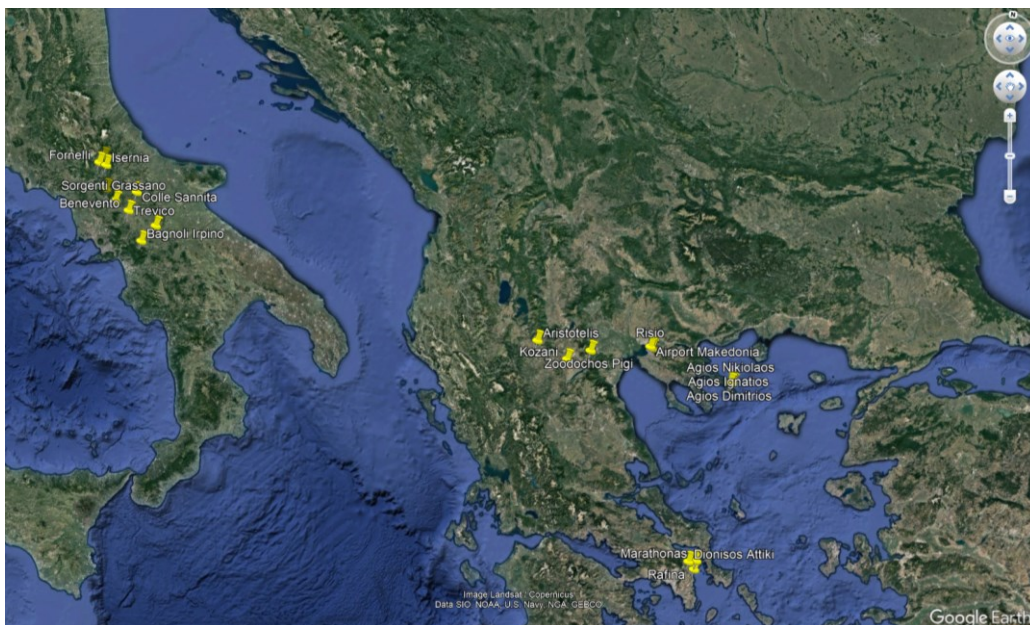


Figure 5.10 Location of the meteorological stations.

5.5 Vadose zone measurements – Geoelectrical measurements

For the vadose zone measurements were established in Anthemountas and Marathonas basin ceramic cups for the monthly collection of water from the vadose zone (**Figure 5.11**). The collectors were placed in depths 0.5, 1, 1.5, 2 and 2.5 meters (**Figure 5.12**). Unfortunately, we couldn't collect the required water to obtain the required analysis mainly due to the hydrogeological characteristics (e.g. clay material) of the vadose zone and the low precipitation (**Figure 5.13**). To overcome this issue and determine the recharge regime, we changed the measurement plan of geoelectrical measurements. We focused the geoelectrical measurements in one site with the most intensive problem of groundwater depletion (Anthemountas basin) (**Figure 5.14**). The monthly measurements couldn't provide valuable information and were essential for high-frequency measurements and coupling with measurements such as soil temperature and moisture for the correction of resistivity anomalies. For the period of September 2021 to December 2023 (the measurements will be continued and after the end of the project's end) we establish a field laboratory in Anthemountas basin with an ERT line of 10 m (**Figure 5.14**), a meteorological station and a rain collector (**Figure 5.15**), a ceramic probe measuring soil moisture and temperature every 10 cm with a depth up to 1 m (**Figure 5.16**). The geoelectrical measurements are obtained every 4 hours, while the probe measures every 30 minutes the moisture and the temperature. The rainfall station provides detailed measurements within the site, while the rainwater is analyzed monthly (e.g. stable isotopes). In the site obtained failing tests and soil texture analysis up to 2 meters in depth to support the geoelectrical measurements.



Figure 5.11 Drilling in the vadose zone for the establishment of the ceramic cups.



Figure 5.12 Upper part of the ceramic cups.



Figure 5.13 Process to collect water from the ceramic cups.

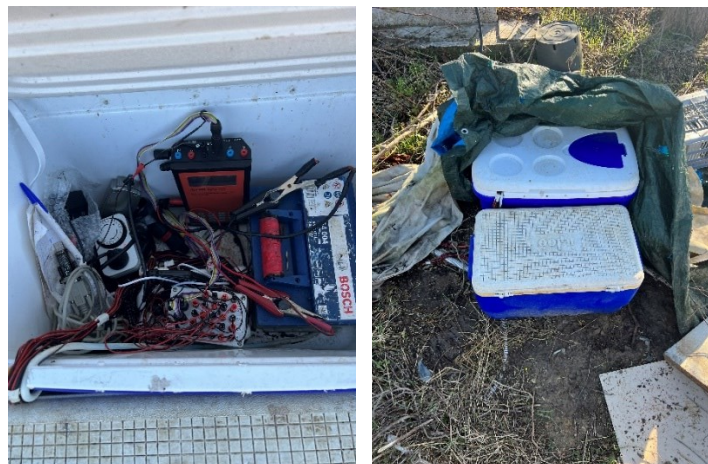


Figure 5.14 Instruments for ERT measurements in N. Risio station.



Figure 5.15 Meteorological and rainwater collector in N. Risio station.



Figure 5.16 Probe for soil moisture and temperature.

6 1st Article in scientific journal

The first article was published in the journal of Water Resource Management with title: **Simulating future groundwater recharge in coastal and inland catchments.** (<https://link.springer.com/article/10.1007/s11269-021-02907-2>). The manuscript constitutes the implementation base of project (**Figure 6.1**). In the manuscript the main tool of the project is presented which is the model ARCSWAT for the estimation of groundwater recharge. The full manuscript is presented in the Annex of the report.

Water Resources Management (2021) 35:3617–3632
<https://doi.org/10.1007/s11269-021-02907-2>



Simulating Future Groundwater Recharge in Coastal and Inland Catchments

Gianluigi Busico^{1,2} · Maria Margarita Ntona^{1,2} · Sílvia C. P. Carvalho³ · Olga Patrikaki⁴ · Konstantinos Voudouris¹ · Nerantzis Kazakis¹

Received: 24 February 2021 / Accepted: 7 July 2021 / Published online: 31 July 2021
© The Author(s), under exclusive licence to Springer Nature B.V. 2021

Figure 6.1 Title page of the 1st publication in the framework of the project.

7 Conclusions

Within this report the general characteristics of the four case studies of GRecoDAM project are presented. Additionally, the results of DRONE application in the case studies are presented, along with the material of the data base and network (deliverables D2-1 and D2-2). The field data collection will be continued in the next steps of the project and will be used as supplement to the material of the modeling process. Finally, all milestones included in the Work Package 2 have been achieved, i.e., the "Monitoring network (M2.1)" and the "Start of field work (M2.2)".

8 References

- Rice, E.W., Baird, R.B., Eaton, A.D., Clesceri, L.S., 1999. Standard Methods for the Examination of Water and Wastewater. American Water Works Association /American Public Works Association/Water Environment Federation.
- USGS (2015) National field manual for the collection of water-quality data.
- U.S.G.S. (2015) variously dated, National field manual for the collection of water-quality data: U.S. Geological Survey Techniques of Water-Resources Investigations, book 9, chaps. A1-A10

ANNEX



Simulating Future Groundwater Recharge in Coastal and Inland Catchments

Gianluigi Busico^{1,2} · Maria Margarita Ntona^{1,2} · Sílvia C. P. Carvalho³ · Olga Patrikaki⁴ · Konstantinos Voudouris¹ · Nerantzis Kazakis¹

Received: 24 February 2021 / Accepted: 7 July 2021 / Published online: 31 July 2021
© The Author(s), under exclusive licence to Springer Nature B.V. 2021

Abstract

Groundwater is a primary source of drinking water in the Mediterranean, however, climate variability in conjunction with mismanagement renders it vulnerable to depletion. Spatiotemporal studies of groundwater recharge are the basis to develop strategies against this phenomenon. In this study, groundwater recharge was spatiotemporally quantified using the Soil and Water Assessment Tool (SWAT) in one coastal and one inland hydrological basin in Greece. A double calibration/validation (CV) procedure using streamflow data and MODIS ET was conducted for the inland basin of Mouriki, whereas only ET values were used in the coastal basin of Anthemountas. Calibration and simulation recharge were accurate in both sites according to statistical indicators and previous studies. In **Mouriki basin**, mean recharge and runoff were estimated as 16% and 9%, respectively. In **Anthemountas basin** recharge to the shallow aquifer and surface runoff were estimated as 12% and 16%, respectively. According to the predicted RCP 4.5 and 8.5 scenarios, significant variations in groundwater recharge are predicted in the coastal zone for the period 2020–2040 with average annual recharges decreasing by 30% (RCP 4.5) and 25% (RCP 8.5). Variations in groundwater recharge in the inland catchment of Mouriki were insignificant for the simulated period. Anthemountas basin was characterized by higher runoff rates. Groundwater management in coastal aquifers should include detailed monitoring of hydrological parameters, reinforced groundwater recharge during winter and reduced groundwater abstraction during summer depending on the spatiotemporal distribution of groundwater recharge.

Keywords SWAT · Data scarcity · Climate model projections · MODIS · Water Resource Management

✉ Nerantzis Kazakis
kazakis@geo.auth.gr

¹ Department of Geology, Laboratory of Engineering Geology & Hydrogeology, Aristotle University of Thessaloniki, 54124 Thessaloniki, Greece

² Department of Environmental, Biological and Pharmaceutical Sciences and Technologies, University of Campania “Luigi Vanvitelli”, Via Vivaldi 43, 81100 Caserta, Italy

³ CCIAM (Climate Change Impacts Adaptation & Modelling)/cE3c, Faculty of Sciences, University of Lisbon, Lisbon, Portugal

⁴ Decentralized Administration of Macedonia-Thrace, Water Directorate, 55134 Thessaloniki, Greece

1 Introduction

The phenomenon of water scarcity in conjunction with the continuous depletion of groundwater resources could seriously threaten the sustainability of natural ecosystems and, consequently, human health and activities (Aeschbach-Hertig and Gleeson 2012). In the last decades, surface waters and groundwater resources have become highly vulnerable due to increased water demands arising from: i) population growth, ii) expanding industrialization, iii) increased food production, iv) anthropogenic pollution, and v) climate variability and land-use change (McDonald et al. 2014).

Consequently, an effective water resource management plan requires the assessment of all relevant hydrological processes, including streamflow, recharge and evapotranspiration. This allows aquifer recharge to be spatiotemporally quantified and suitable zones for sustainable groundwater exploitation be identified at basin scale. Several studies have pointed out the necessity of reliable groundwater recharge estimates to optimize groundwater and surface water exploitation (Nyeko 2014). The evaluation of recharge is essential in regions with significant climatic variations which can impact watershed hydrology and potentially lead to seasonal reduction of fresh water availability (Carvalho-Santos et al. 2017). However, recharge rate is characterized by discrepancies in space and time due to differences in local geomorphology, climate and vegetation (Scanlon et al. 2002). The Mediterranean region is one of the most vulnerable zones worldwide due to the magnitude of predicted changes to its temperature and rainfall patterns (Giorgi & Lionello 2008). Such variabilities could influence the hydrogeological regime and cause significant variations in the quantity and quality of groundwater resources (Donnelly et al. 2017).

Several methodologies have been developed and tested to estimate groundwater recharge and evaluate hydrological variation driven by climate and land use changes, such as: i) the paired catchments approach (Van Loon et al. 2019), ii) time series analysis (Hawtree et al. 2015), and iii) hydrological modeling. The latter can provide the most robust structure to analyze the complex relationships between climate, human activities and water resources as it accounts for the spatial variability of the specific factors influencing groundwater recharge (Awan et al. 2014). Physically based and distributed hydrological models have proved to be an important tool for water resource management (Li et al. 2009). Additionally, due to increasing availability of global and regional datasets, their applicability has been greatly enhanced (Abbaspour et al. 2019). The Soil and Water Assessment Tool (SWAT, Neitsch et al. 2000) is a watershed-scale, physically based, distributed hydrological model, that was created to evaluate and predict the impact of different agricultural management practices on hydrological processes and water quality status (Arnold et al. 1998). The SWAT model is considered a valuable tool to assess the effects of climate and land use changes on all basin hydrological processes such as: streamflow, soil erosion and recharge (Busico et al. 2020). Precise calibration, validation and uncertainty analysis is required to achieve the best model performance and reliability. Values of river/torrent streamflow are normally used for model calibration. Unfortunately, these parameters are not widely available thus making calibration problematic, especially in ungauged basins. To overcome this issue, many studies have demonstrated the potential of calibration using remotely sensed evapotranspiration (ET). Moderate Resolution Imaging Spectroradiometer (MODIS) ET products have proven to be reliable and useful tools for hydrological studies. These products are free downloadable datasets that are relatively simple to use (Miranda et al. 2017). Parajuli et al. (2018), assessed how a SWAT calibration with ET could adequately simulate streamflow data, while Odusanya et al. (2019),

highlighted the main advantages of a double SWAT calibration using streamflow and ET data. Accordingly, ET measurements become essential when calibrating a SWAT model, especially in an ungauged basin where a water resource management plan is necessary to ensure groundwater sustainability (Nyeko 2014). The SWAT model has been widely used in the Mediterranean, and especially in Greece (Venetsanou et al. 2020; Gemitzi et al. 2017). The SWAT model was selected to investigate spatiotemporal groundwater variation caused by climatic variations in two basins in northern Greece. Anthemountas basin is a coastal catchment where the water demands for human activities are met completely by local groundwater resources. Groundwater overexploitation in this coastal area has caused a significant lowering of the water table and groundwater salinization. In the inland basin of Mouriki, the aquifer is used mainly to meet the water demands for local domestic and agricultural use and has been subjected to increasing pressure in recent years.

The evaluation of future trends and spatiotemporal variations of groundwater recharge rates is of outmost importance in the Mediterranean region for sustainable groundwater resources management. Nevertheless, the lack of relevant data requires examining different approaches to calibrate and verify modelling processes. Such approaches should consider different hydrogeological environments, such as those examined in the present work (one coastal and one inland aquifer). However, despite the importance of this issue, few studies have focused on the spatiotemporal variation of groundwater recharge. Sutanudjaja et al. (2018), proposed a spatial distribution of recharge on continental and regional scale by sacrificing spatial resolution. Several studies have applied the SWAT model for local assessment, focusing only on spatial (Awan and Ismael 2014) or temporal recharge (Gemitzi et al. 2017).

In this study, we aim to estimate the spatiotemporal variation of groundwater recharge at basin scale. To ensure result robustness different calibration approaches were used in two basins with different hydrogeological regimes. The innovative results of this study could be used as a fundamental framework to estimate spatiotemporal variation of groundwater recharge in areas with limited hydrological data.

2 Study Areas

2.1 Mouriki Basin

The Mouriki basin is located in the north part of Kozani Prefecture in northern central Greece (Fig. 1). It is an inland basin with a surface area of 110 km². The mean altitude of the study area is 874.5 m a.s.l. with a mean slope inclination of 26.1%. The climate is semi-arid Mediterranean with moderate rainfall during summer. The average annual air temperature and precipitation values are 11.2°C and 636 mm, respectively (Patrikaki 2012). The geological setting of the study area is presented in the Supplementary Material (Fig. S1a).

The main aquifer system is hosted in alluvial deposits with a mean thickness of 70 m covering an area of 30.5 km². The groundwater flow follows the local morphology moving towards the lowlands in an SSW to NNE direction. Livestock and agriculture are the main activities in the area and the main cultivations are corn, cereal crops, fruit trees, vegetables and legumes. The mountainous part of the basin is covered with mixed, coniferous forest vegetation.

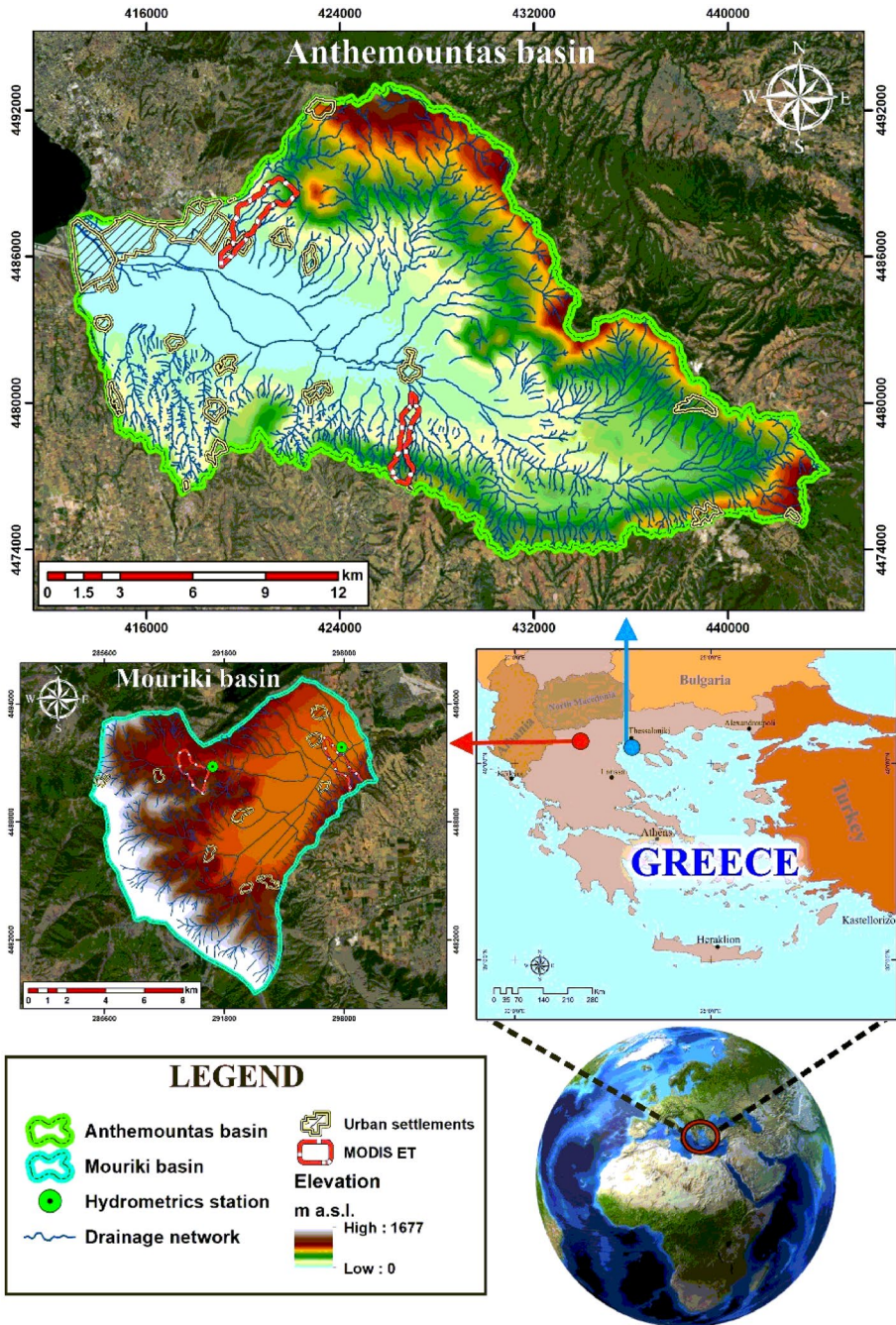


Fig. 1 Location of the study areas

2.2 Anthemountas Basin

Anthemountas basin is a coastal basin located in the eastern part of Thermaikos Gulf in northern Greece (Fig. 1b). The basin covers an area of 374 km², with altitudes ranging from 0 m (coastal zone) to 1201 m a.s.l (Mount Hortiatis). The mean slope inclination is 20% and ranges from 0.1 to 40%. The climate is characterized as a typical Mediterranean semi-arid climate with dry summers and wet winters. The mean annual temperature and precipitation values are 15.1 °C and 575 mm, respectively. The geological setting of Anthemountas basin is presented in the Supplementary Material (Fig. S1b).

The basin is characterized by a multiple aquifer system consisting of various aquifer types: i) a porous aquifer hosted in the Quaternary and Neogene sediments, ii) a karst aquifer located in the south-central part of the basin, and iii) fractured rock aquifers in the mountainous part of the basin. Agriculture is the primary economic activity of the area, although tourism has increased in recent years, mainly during the summer. The area's main crops include vegetables, olives, wine grapes, corn and cereals. The area's growing domestic and irrigation water requirements are met by numerous boreholes located in the porous aquifers. Due to overexploitation, groundwater depletion has been observed in the aquifer. There is limited surface runoff data for this study site.

3 Materials and Methods

The assessment of groundwater recharge variations and their relationship with other hydrological parameters requires various hydrological and hydrogeological data. The SWAT model was applied to both study areas. A brief resume of SWAT theory is available in the Supplementary Materials. A double calibration/validation (CV) procedure using streamflow data and MODIS ET was conducted for Mouriki basin, whereas only ET values were used in Anthemountas basin due to the complete lack of hydrometric data for this site. The assessment was performed using real (non-predicted) meteorological data for the period 2000–2019 and predicted data for the future (2019–2040) under two emission scenarios (RCP 4.5 and 8.5).

3.1 Data Collection

The data necessary to perform satisfactory hydrogeological evaluations of the two catchment basins was obtained and collected from online free-access sources, field measurements and relevant literature (Table S1). Specifically, i) a Digital Terrain Model (DTM) with a 10×10 m cell resolution was used to define the main watershed features, ii) soil information was obtained from the Digital Soil World Map (DSMW FAO 2007; scale 1:5 million) and amended with field measurements and default SWAT database values, iii) a preliminary land use classification was made using Corine Land Cover (CLC) classes for the year 2018 and then discretized using satellite images and relevant literature, and iv) meteorological data of minimum and maximum daily temperature and precipitation values for a 25-year period (1996–2020) were obtained from three meteorological stations and analyzed in the

R programming environment to complete any missing data. Data from two meteorological stations (Aristotelis and Kozani) were used for Mouriki basin and one station (Makedonia airport) for Anthemountas basin. Methods of elevation bands were used to reproduce the precipitation variability within the basins due to orographic effects. This methodology has been proved to greatly enhance model reliability even utilizing point observed precipitation (Tuo et al. 2016).

Data on daily river discharge and monthly ET values were used for the model calibration/validation (CV). Discharge data was obtained from two hydrometric monitoring stations (Galatia and Variko) located within [Mouriki basin](#) for the period November 2004 to September 2007 (Fig. 1). Monthly ET values for 2002–2010 for both Mouriki and Anthemountas basins were sourced from the MODIS dataset. The MOD16A2 Version 6 Total ET product (including potential and real ET) is an 8-day composite dataset produced at 500×500 m pixel resolution. The data was download using the AppEEARS (AppEEARS 2020) interface and the MYD16A3GF model (Running et al. 2019). Specifically, the algorithm used in the MOD16 products is based on the Penman–Monteith equation, which includes inputs of daily meteorological data along with MODIS remotely sensed data products such as vegetation property dynamics, albedo and land cover (Mu et al. 2011). The ET data was extracted using the average spatial values of two internal sub-basins within the two study areas (Fig. 1). The historical climate data and future projections for the entire period of 1976–2040 focused on simulations performed by the GCM/RCM combination, entitled MPI-M-MPI-ESM-LR/MPI-CSC-REMO2009, and here called REMO, made available by the World Climate Research Programme's CORDEX initiative (www.euro-cordex.net).

4 Modelling Framework

A detailed analysis of the SWAT calibration and performance evaluation procedure is presented in the Supplementary Material and includes equations, the monitoring stations (Fig. S2c), and the statistical methods applied to evaluate the modeling results.

The regimes of recharge, streamflow and evapotranspiration for the two analyzed catchments areas were obtained by following four main steps (Fig. 2): i) the physical characteristics of morphology, land cover and soil were collected and used as main inputs for the SWAT set-up, ii) the real (non-predicted) meteorological data were used to run the model for a 10-year period from 2000 to 2010, iii) the model was then calibrated and validated for Mouriki basin using observed streamflow and evapotranspiration data and using evapotranspiration for Anthemountas basin, and iv) the SWAT model used the selected RCM to simulate the past time period of 2000–2020 and the future period of 2020–2040 under two different emission pathways (RCP 4.5 and 8.5). The results were then analyzed to obtain annual values of recharge, streamflow and evapotranspiration using a time series chart. To obtain a spatial/temporal representation of aquifer recharge in both areas, the average yearly recharge (mm) over a 20-year period (2020–2040) was estimated at basin scale and compared with the 5-year sub-basin recharge for the shorter periods 2021–2025, 2026–2030, 2031–2035, and 2036–2040. This elaboration was performed considering only the 4.5 scenario since it is considered the most reliable of the two.

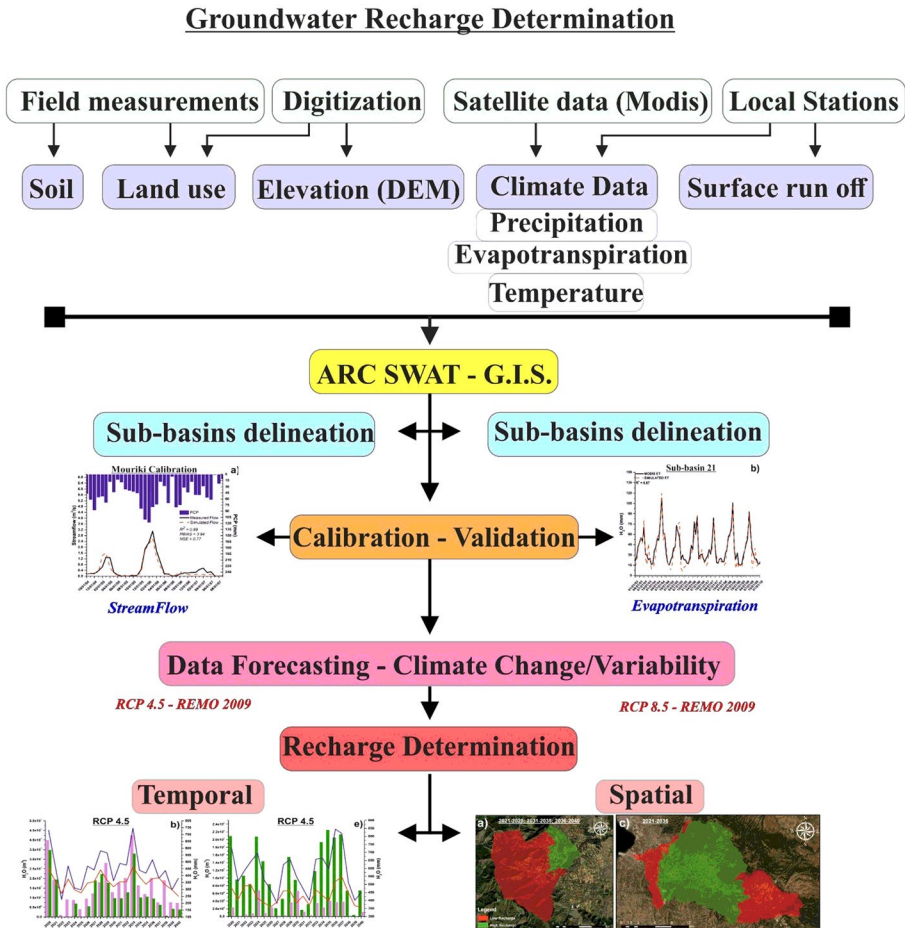


Fig. 2 Flowchart of the process followed to estimate spatiotemporal groundwater recharge

5 Results

5.1 SWAT Application

The application of SWAT in Mouriki and Anthemountas basins was done using ArcSWAT 2012 in an ArcGIS 10.5 environment. Mouriki basin was divided into 149 sub-basins and a total of 500 HRU. The area is mainly agricultural (Fig. S2a), dominated by wheat and vegetable crops (mainly tomatoes and potatoes) that cover 70% of the territory. Urban settlements account for less than 2% of the site’s surface and the remaining areas are covered by dense pine and oak forests. According to the DSWM, the entire basin is characterized by Chromic Luvisols with a clay-loam texture and a hydraulic conductivity (K_s) of 7.68 mm/h (Fig. S2b). The Anthemountas basin was divided into 233 sub-basins retaining a maximum of 500 HRU (Fig. S3c). The maximum of 500 HRU was set to reduce the model’s spatial requirements and computational time in accordance with Busico et al. (2020). The

analysis showed that land use of Anthemountas basin was mainly agricultural. Over 50% of the basin is cultivated with crops including wheat, corn, olives and vegetables (mainly lettuce and carrot), while urban settlements account for 6% of the basin's surface area and are mainly located along the coast (Fig. S3a). The remaining territory is characterized by Mediterranean shrubland and oak forests interspersed with pasture. In both catchments, multiple land uses were established by using the HRU refinements tool to reproduce high crop heterogeneity (Figs. S2a and S3a) and reflect the different forest densities in both study areas.

Two soil categories were identified in Anthemountas basin following the DSMW classification: i) Chromic Luvisols in the central and eastern parts of the basin with the same characteristics as those of Mouriki basin, and ii) Calcaric Regosols with a clay-loam texture and a K_s of 4.2 mm/h that occur in the western part of the site and near the coastal zone. Morphologically, both catchments were divided into four slope classes with a 5% interval (Figs. S2b and S3b). Hargreaves method was applied to calculate ET calculation due to the lack of climatic data.

5.2 SWAT Calibration and Validation

The CV procedure was performed using real climatic data for the period 1996–2010 obtained from the local meteorological stations. A double parameter calibration was conducted for Mouriki basin using monthly streamflow data and MODIS monthly ET values via SWAT-CUP standalone software choosing the SUFI-2 algorithm. In Anthemountas basin the CV procedure was performed using only the MODIS values of ET and Mouriki's calibration results as a general guide, due to the complete absence of streamflow and runoff monitoring stations. The calibration parameters were chosen after an extensive review of the relevant literature. Following Chen et al. (2019), nine parameters were identified as those most relevant in affecting streamflow and ET simulation (Table S2). The NSE index was selected as optimization function for the SUFI-2 algorithm along with the statistical indices PBIAS and coefficient of determination (R^2) to check the model's performance. The boundary values of Moriasi et al. (2007) were considered to evaluate the reliability of the model's results. Due to the limited range of available streamflow data, data from the hydrometric station of Variko (basin outlet) were used for the calibration in the Mouriki analysis, while data from Galatia station (internal station) were checked for the validation procedure using the same time period. A total number of 1000 calibration runs divided into two interactions of 500 runs each were performed for the simulation. The first interaction set-up was applied using the initial boundaries (min. and max. columns in Table S2) as proposed by Abbaspour (2015). Figure S4 presents the results of the CV procedure applied for both study sites. According to the statistical indices values, the streamflow calibration showed excellent performance with R^2 0.89, PBIAS 3.94, and NSE 0.77 (Fig. S4a). Following the streamflow calibration, the SWAT-calculated ET values for sub-basin 21 were compared with the mean spatial ET values obtained from MODIS. The results of the comparison are shown in Fig. 4b and show a good match between SWAT and MODIS ET (R^2 0.87). The final parameter fitted values are shown in Table S2 along with the results of the sensitivity analysis (P-value). Galatia station (streamflow) and sub-basin 42 (ET) were checked for validation. In this case, the three indices also showed remarkable performance (R^2 0.83, PBIAS 25 and NSE 0.8 for streamflow, and R^2 0.87 for ET). In Anthemountas basin an alternative calibration was selected due to the complete lack of streamflow data. ET is the main parameter of the

hydrological cycle and can be used to estimate other components of the water balance, including surface runoff, lateral flow, base flow and aquifer recharge. The calibration parameters were the same as those applied in the case of Mouriki basin. Four parameters were detected as sensitive for ET simulation in [Anthemountas basin](#): a) the fraction of recharge to the deeper aquifer (RCHRG_DP), b) the soil evaporation compensation factor (ESCO), c) the threshold depth of water in the shallow aquifer (GWQMN), and d) the revap coefficient (GW_REVAP). All final parameter values are presented in [Table S4](#). Calibration with average ET values from MODIS for sub-basin 39 ([Fig. S4e](#)) showed an acceptable trend with an R^2 of 0.86, while validation for sub-basin 177 resulted in an R^2 of 0.83 ([Fig. S4d](#)).

5.2.1 Groundwater Balance

Following the CV procedure, conducted with the available real (non-predicted) climate data, the SWAT model was run for the period 1996–2040 (4-year warm-up) using the historical/projected climate dataset for the two catchments to evaluate variations of the main parameters of the hydrological cycle in the short-term period. For this purpose, a subset of climate models was selected considering the simulations made available by the World Climate Research Program's CORDEX initiative. Different criteria were considered including a wide range of possible future projections, a variety of driving global climate models (GCM), and several institutions providing regional climate models (RCMs). Nevertheless, to limit the necessary computational efforts for further processing using the SWAT model, the climate projections of this study focused on the simulations from a GCM/RCM combination entitled MPI-M-MPI-ESM-LR/MPI-CSC-REMO2009, and here called REMO. [Jacob et al. \(2012\)](#) state that REMO performs best for temperature over Europe, the Mediterranean and north America, whereas high skill scores for rainfall are produced in the regions of Africa, western Asia and the Mediterranean. The REMO model was also highlighted by [Nerantzaki et al. \(2019\)](#) for its accuracy when studying climate change impacts on the hydrological processes of the island of Crete. Regarding future climate scenarios, projections were based on two Representative Concentration Pathways: RCPs 4.5 and 8.5 (scenarios that include time series of emissions and concentrations of the full suite of greenhouse gases, aerosols, and chemically active gases, as well as land use). While RCP 4.5 is an intermediate stabilization pathway in which radiative forcing is stabilized at approximately 4.5 W/m^2 , RCP 8.5 reaches greater than 8.5 W/m^2 by 2100 and continues to rise for some amount of time ([Moss et al. 2008](#)). Variations in the hydrological parameters over time, considering the actual data and the two predicted future scenarios are shown in [Fig. 3](#). The results obtained for the long-term mean annual water balance are in good agreement with those of previous studies on Mouriki ([Patrikaki 2010](#)) and Anthemountas ([Kazakis 2013](#)) basins.

5.2.2 Mouriki basin

The total average annual ET in [Mouriki basin](#) was calculated as accounting for 75% of the hydrological balance, while recharge and runoff account for 16% and 9%, respectively. Mean annual recharge for the period 2000–2019 was calculated to be $12.4 \times 10^6 \text{ m}^3$ while runoff was much lower with an average value of $3.00 \times 10^6 \text{ m}^3$ per year. A high inverse correlation between recharge and ET was estimated. The simulation for 2020–2040 under the

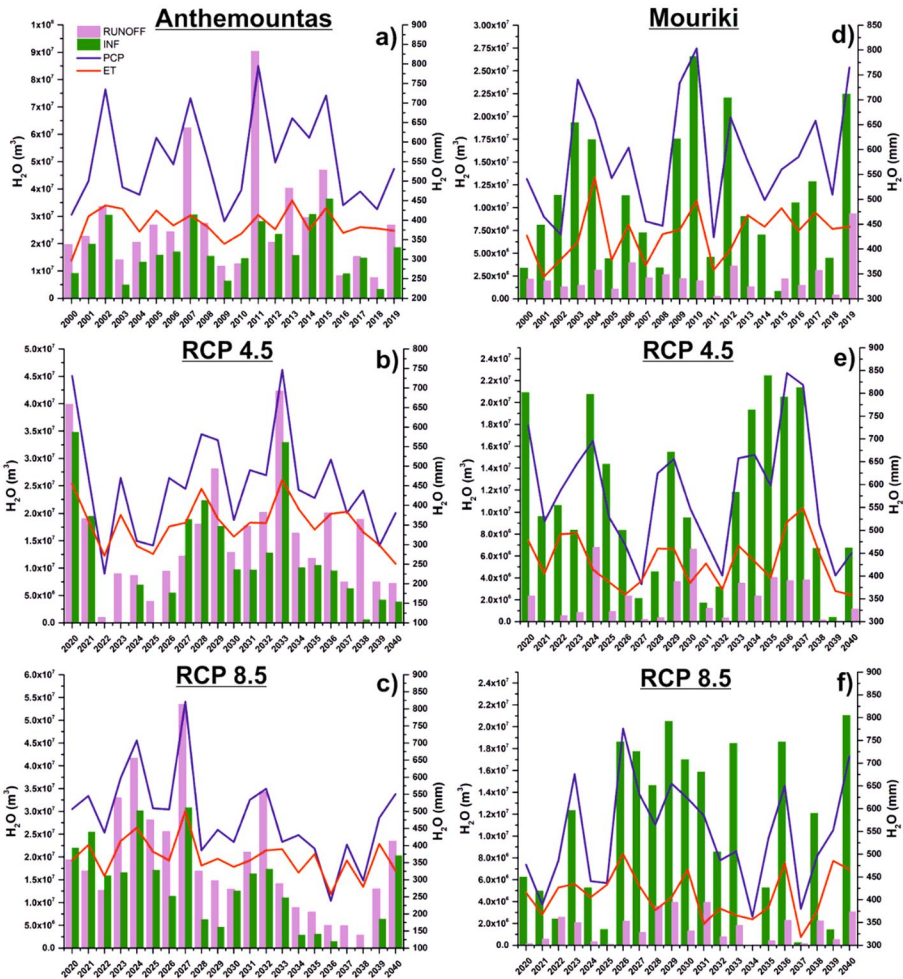


Fig. 3 Water balance representation for the two study areas considering the actual scenario and the two predicted future scenarios

RCP 4.5 and 8.5 scenarios (Fig. 3b, c) did not predict significant differences in the average percentages of the examined parameters. Indeed, a 25% decrease in runoff was predicted for the RCP 8.5 scenario. The relation between recharge and ET remained constant in both predicted RCP scenarios. The total amount of infiltration is not predicted to decrease significantly but is predicted to experience annual variations in the future.

5.2.3 Anthemountas Basin

For the period 2000–2019, total ET was estimated to account for 72% of the entire hydrological balance in **Anthemountas basin**, while recharge to the shallow aquifer and surface runoff RF accounted for 12% and 16%, respectively (Fig. 3d). Mean annual recharge to the shallow aquifer was calculated as $17.9 \times 10^6 \text{ m}^3$, while runoff was $28.1 \times 10^6 \text{ m}^3$. The runoff/recharge ratio appears stable for 2000–2019 thus confirming the strong relationship


between the two parameters. According to the predicted RCP 4.5 and 8.5 scenarios, greater variation will characterize the years 2020–2040 and the average annual recharge will decrease by 30% (RCP 4.5) and 25% (RCP 8.5). Both climate scenarios predict severe drought conditions due to low precipitation and high ET rates which will negatively affect both recharge and runoff values. Runoff values are predicted to reduce by 30% and 25% for the RCP 4.5 and 8.5 scenarios, respectively, but remain consistently higher than recharge values.

5.2.4 Groundwater Recharge Discretization

Following the RCP 4.5 scenario, the 20-year average recharge values for 2020–2040 were predicted as being 87 mm and 40 mm for Mouriki and Anthemountas basins, respectively. To identify the most sensitive sub-basins in both study areas, a 5-year average recharge value was calculated for each sub-basin for four stress periods (2021–2025, 2026–2030, 2031–2035, 2036–2040). The sub-basins were then classified as “Low recharge” or “High recharge” when the mean recharge value of each stress period was lower or higher than the mean recharge value of the total time period. In this way, spatial mapping of future recharge trends was achieved (Fig. 4). The higher recharge areas of Mouriki basin are concentrated near the basin’s outlet where the morphology is flat. Consequently, all the mountainous areas characterized by steeper reliefs and higher runoff, showed a 5-year average recharge of under 87 mm. No significant changes over time were identified during the four stress periods. However, one exception is predicted to occur in the years 2026–2030 where a 10% increase is observed in the areas of “High recharge”. These areas were previously classified as “Low Recharge”. A different situation is observed in the Anthemountas catchment basin. The first three stress periods showed stable classification, with the central part of the basin classified as “High recharge”. For the last stress period of 2026–2030, the entire basin is predicted to show an average recharge of under 40 mm.

6 Discussion

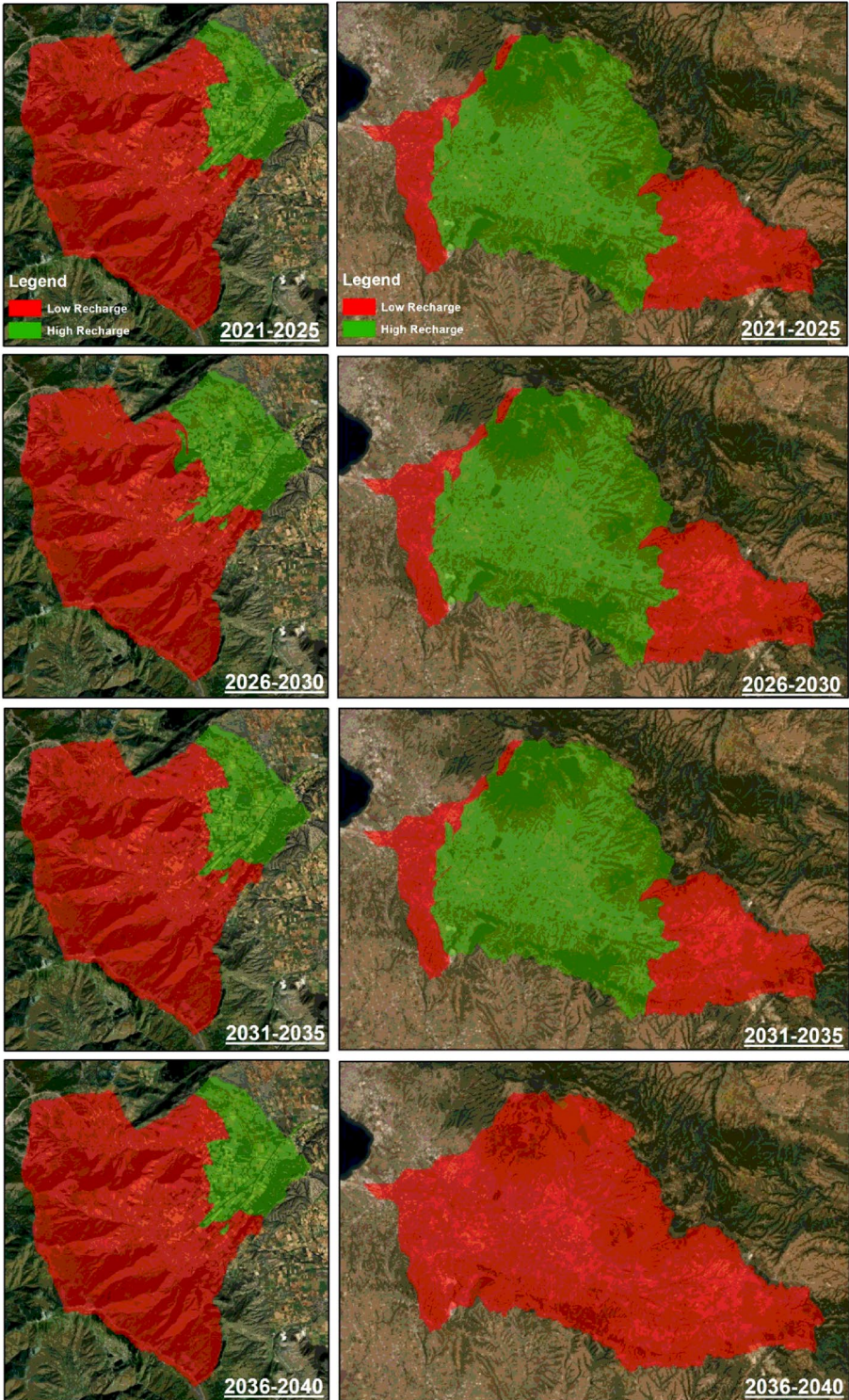
Climate projections for the Mediterranean region predict an estimated annual increase in temperature of between 1.5 and 2.0 °C, especially during the summer period (Giorgi and Lionello 2008; Bucchignani et al. 2016). In contrast, a slight decrease in precipitation is predicted with a marked seasonal regime (Mastrocicco et al. 2019) together with increased frequency of extreme events (Busico et al. 2019). In the present study the SWAT model was successfully calibrated using streamflow and ET to forecast surface runoff and groundwater recharge in two Mediterranean basins. The robustness of the SWAT model was verified using the existing groundwater balance, which highlights the importance of the basic hydrogeological research that must be supported by a detailed monitoring plan of the various hydrological components. The two hydrological basins showed different situations and very different predicted responses to climatic change. Despite showing a similar ET percentage and comparable mean annual precipitation values for the simulation period, they greatly differ in runoff and groundwater recharge. These differences were observed inside the catchments and can be attributed to two main characteristics: i) basin land cover, and ii) rain distribution throughout the year. Regarding land cover, Mouriki basin has a higher percentage of high-altitude dense pine forests than

Fig. 4 Spatial distribution of “High” and “Low” recharge areas in the two catchment basins 

Anthemountas basin in which pine forests represent just 2% of the total forested land. Moreover, the main forest vegetation of the Anthemountas catchment is sclerophyllous (oak) and Mediterranean shrub-land usually interspersed with pastureland of low tree density that can benefit runoff formation (Zhang et al. 2020). Agricultural land covers a much higher percentage in Anthemountas than Mouriki basin. This explains the higher runoff values observed in this site compared to the recharge values. These results are in accordance with studies that suggest susceptibility to runoff in agricultural and sparsely forested areas is generally higher than in densely forested areas where runoff is reduced to the benefit of evapotranspiration and infiltration (Ferreira et al. 2012). The runoff regime might be higher due to increased land cover with low permeability potential (Eshtawi et al. 2014). Moreover, analysis of the meteorological data showed that Anthemountas basin has 30% less rain days than Mouriki, despite the mean annual precipitation for the studied period being almost the same for both sites, thus indicating higher precipitation density in Mouriki basin (Table S3).

The spatial distribution of groundwater recharge indicated that a severe water crisis may occur in Anthemountas basin in the years 2036–2040. A decrease in precipitation along with an increase in ET (Fig. 4e) may be the main causes of this crisis, while groundwater scarcity may be higher if the 8.5 scenario is confirmed. In contrast, the predictions for Mouriki basin indicate a more stable groundwater recharge regime for the next 20 years. The decrease in recharge predicted by the climate scenario simulation for Anthemountas basin agrees with the conclusions of Tylor et al. (2013) who predicted a substantial reduction in potential groundwater recharge in the future for all southern Europe. On the other hand, the results of that study confirmed that RCH can be slightly subjective to spatial variability (Jyrkama and Sykes 2007). The future recharge projection for Anthemountas basin predicts a serious threat on water availability in both RCP 4.5 and 8.5 emission scenarios. For this reason, an extensive monitoring system should be set up inside the basin, including groundwater level monitoring, surface run off measurements, and climatological stations. Some countermeasures such as the construction of reservoirs to collect runoff water or land use management that targets higher infiltration could be also considered for inclusion in future water resources planning. In coastal aquifers where groundwater constitutes the main water supply source any management plans should be adopted based on the simulation results. Groundwater depletion and water table decline intensifies due to increasing water demands. Initially, the phenomenon should be stabilized by reinforcing groundwater recharge and limiting groundwater abstraction. Additionally, small dams could be transformed into small power plants and excess water collected in winter used to manage aquifer recharge.

Future research should aim to apply this SWAT simulation methodology to other catchment basins in the Mediterranean, and compare the results and limitations of this technique. Specifically, combining surface/groundwater modelling will allow the more accurate simulation of all water cycle components and help to account for different climatic and management scenarios such as: i) droughts, ii) extreme rainfall events, and iii) groundwater overexploitation. At present, the main limitations of this study include data scarcity due to the lack of monitoring stations. Nevertheless, despite the absence of hydrological monitoring, data can be partly obtained by advanced technological innovation (e.g., satellite data), although ground stations and monitoring remain



an essential factor for effective water resource management and reliable predictions. Adaptive strategies and multi-data elaboration are required to overcome past decades of groundwater mismanagement.

7 Conclusions

The hydrological physical-based model SWAT was applied in two catchment basins of northern Greece, Mouriki and Anthemountas, to forecast groundwater recharge under climate-driven changes. Due to the absence of hydrometric stations in [Anthemountas basin](#), the calibration was successfully obtained by using ET values from MODIS. The two study areas differ widely regarding recharge and runoff predictions. Mouriki is characterized by a high recharge rate and low runoff production that will probably not undergo significant changes in the future, both in temporal and spatial distributions. The recharge of this site is highly dependent on ET and driven by the local dense forest vegetation. In [Anthemountas basin](#), runoff was calculated as being significantly higher than recharge. This difference is attributed to land cover regime and precipitation levels. In the coastal basin of Anthemountas, the predicted reduction in precipitation and increased air temperatures may lead to years with severe drought conditions in the future. This is in accordance with predicted decrease in groundwater recharge which may lead to groundwater scarcity in the coming years, especially for the period 2036–2040. Small eco-friendly energy recharge dams may be a solution to partly overcome future groundwater scarcity in [Anthemountas basin](#).

Supplementary Information The online version contains supplementary material available at <https://doi.org/10.1007/s11269-021-02907-2>.

Acknowledgements This research project was supported financially by the Hellenic Foundation for Research and Innovation (H.F.R.I.) under the “Second Call for H.F.R.I. Research Projects to support Post-Doctoral Researchers” (Project Number: 00138, Title: Groundwater Depletion. Are Eco-Friendly Energy Recharge Dams a Solution?). The scholarship and research activities of Maria Margarita Ntona were part of the Environment, Design and Innovation PhD Program funded by the V:ALERE 2020 Program (VANviteLLi pEr la RicErca) of the University of Campania “Luigi Vanvitelli”.

Author Contributions Conceptualization, G.B. and N.K.; methodology, G.B., M.M.N., S.C.; software, G.B., M.M.N., N.K.; formal analysis, G.B., N.K., K.V.; investigation, M.M.N., P.O., N.K.; data curation, G.B., M.M.N., S.C.; writing—original draft preparation, G.B., M.M.N.; writing—review and editing, N.K., K.V.; supervision, N.K., K.V. All authors have read and agreed to the published version of the manuscript.

Funding The research project was supported financially by the Hellenic Foundation for Research and Innovation (H.F.R.I.) under the “Second Call for H.F.R.I. Research Projects to support Post-Doctoral Researchers” (Project Number: 00138, Title: Groundwater Depletion. Are Eco-Friendly Energy Recharge Dams a Solution?).

Data Availability The datasets generated during the current study are available from the corresponding author on reasonable request.

Declarations

Ethics Approval The authors declare that the submitted manuscript is original and unpublished elsewhere, and that this manuscript complies with the Ethical Rules applicable for this journal.

Conflicts of Interest The authors have no conflicts of interest to declare that are relevant to the content of this article.

References

- Abbaspour KC (2015) Calibration and Uncertainty Programs. SWAT-cup User Manual
- Abbaspour KC, Vaghefi SA, Yang H, Srinivasan R (2019) Global soil, land-use, evapotranspiration, historical and future weather databases for SWAT Applications. *Sci Data* 6:263. <https://doi.org/10.1038/s41597-019-0282-4>
- AppEEARS Team (2020) Application for extracting and exploring analysis ready samples (AppEEARS). Ver. 2.40. NASA EOSDIS Land Processes Distributed Active Archive Center (LP DAAC), USGS/Earth Resources Observation and Science (EROS) Center, Sioux Falls, South Dakota, USA. Accessed May 3, 2020. <https://lpdaacsvc.cr.usgs.gov/appeears>
- Arnold JG, Srinivasan R, Mutiiah RS, Williams JR (1998) Large-area hydrologic modeling and assessment: Part I. Model development. *J Am Water Resour Assoc* 34:73–89
- Aeschbach-Hertig W, Gleeson T (2012) Regional strategies for the accelerating global problem of groundwater depletion. *Nat Geosci* 5:853–861. <https://doi.org/10.1038/ngeo1617>
- Awan UK, Ismaeel A (2014) A new technique to map groundwater recharge in irrigated areas using a SWAT model under changing climate. *J Hydrol* 519:1368–1382. <https://doi.org/10.1016/j.jhydrol.2014.08.049>
- Bucchignani E, Montesarchio M, Zollo AL, Mercogliano P (2016) High-resolution climate simulations with COSMO-CLM over Italy: performance evaluation and climate projections for the 21st century. *Int J Climatol* 36(2):735–756. <https://doi.org/10.1002/joc.4379>
- Busico G, Colombani N, Fronzi D, Pellegrini M, Tazioli A, Mastrocicco M (2020) Evaluating SWAT model performance, considering different soils data input, to quantify actual and future runoff susceptibility in a highly urbanized basin. *J Environ Manag* 266:110625. <https://doi.org/10.1016/j.jenvman.2020.110625>
- Busico G, Giuditta E, Kazakis N, Colombani N (2019) A hybrid GIS and AHP approach for modelling actual and future forest fire risk under climate change accounting water resources attenuation role. *Sustainability* 11:7166. <https://doi.org/10.3390/su11247166>
- Carvalho-Santos C, Monteiro AT, Azevedo JC, Honrado JP, Nunes JP (2017) Climate Change Impacts on Water Resources and Reservoir Management: Uncertainty and Adaptation for a Mountain Catchment in Northeast Portugal. *Water Resour Manag* 31(11):3355–3370. <https://doi.org/10.1007/s11269-017-1672-z>
- Chen Y, Xu CY, Chen X et al (2019) Uncertainty in simulation of land-use change impacts on catchment runoff with multi-timescales based on the comparison of the HSPF and SWAT models. *J Hydrol* 573:486–500. <https://doi.org/10.1016/j.jhydrol.2019.03.091>
- Donnelly C, Greuell W, Andersson J et al (2017) Impacts of climate change on European hydrology at 1.5, 2 and 3 degrees mean global warming above preindustrial level. *Clim Change* 143:13–26. <https://doi.org/10.1007/s10584-017-1971-7>
- Eshtawi T, Evers M, Tischbein To B (2014) Quantifying the impact of urban area expansion on groundwater recharge and surface runoff. *Hydrolog Sci J* 61(5):826–843. <https://doi.org/10.1080/02626667.2014.1000916>
- Ferreira CSS, Ferreira AJD, Pato RL, Magalhaes MC, Coelho CO, Santos C (2012) Rainfall-runoff-erosion relationships study for different land uses, in a suburban area. *Z Geomorphol* 56:5–20. <https://doi.org/10.1127/0372-8854/2012/S-00101>
- Food and Agriculture Organization of the United Nations (2007) Available online at: <http://www.fao.org/geonetwork/srv/en/metadata.show?id%414116>
- Gemitz A, Ajami H, Richnow H (2017) Developing empirical monthly groundwater recharge equations based on modeling and remote sensing data modeling future groundwater recharge to predict potential climate change impacts. *J Hydrol* 546:1–13. <https://doi.org/10.1016/j.jhydrol.2017.01.005>
- Giorgi F, Lionello P (2008) Climate change projections for the Mediterranean region. *Global Planet Change* 63(2–3):90–104. <https://doi.org/10.1016/j.gloplacha.2007.09.005>
- Hawtree D, Nunes JP, Keizer JJ, Jacinto R et al (2015) Timeseries analysis of the long-term hydrologic impacts of afforestation in the Aguedawatershed of north-central Portugal. *Hydrol Earth Syst Sci* 19(7):3033–3045. <https://doi.org/10.5194/hess-19-3033-2015>
- Jacob D, Elizalde A, Haensler A et al (2012) Assessing the Transferability of the Regional Climate Model REMO to Different COordinated Regional Climate Downscaling EXperiment (CORDEX) Regions. *Atmosphere* 3(1):181–199. <https://doi.org/10.3390/atmos3010181>
- Jyrkama MI, Sykes JF (2007) The impact of climate change on spatially varying groundwater recharge in the grand river watershed (Ontario). *J Hydrol* 338(3–4):237–250. <https://doi.org/10.1016/j.jhydrol.2007.02.036>
- Kazakis N (2013) Groundwater Pollution Risk Assessment in Anthemountas Basin. Department of Geology, Aristotle University of Thessaloniki (Ph.D. thesis, in Greek with English summary)

- Li Z, Liu W, Zhang X, Zheng F (2009) Impacts of land use change and climate variability on hydrology in an agricultural catchment on the loess plateau of china. *J Hydrol* 377(1–2):35–42. <https://doi.org/10.1016/j.jhydrol.2009.08.007>
- Mastrocicco M, Busico G, Colombani N, Vigliotti M, Ruberti D (2019) Modelling actual and future sea-water intrusion in the Variconi coastal wetland (Italy) due to climate and landscape changes. *Water (Switzerland)* 11(7). <https://doi.org/10.3390/w11071502>.
- Miranda RDQ, Galvncio JD, Moura MSB et al (2017) Reliability of MODIS evapotranspiration products for heterogeneous dry forest: A study case of caatinga. *Adv Meteorol*. <https://doi.org/10.1155/2017/9314801>
- McDonald RI, Weber K, Padowski J, Flrke M et al (2014) Water on an urban planet: Urbanization and the reach of urban water infrastructure. *Global Environ Chang* 27:96–105. <https://doi.org/10.1016/j.gloenvcha.2014.04.022>
- Moriyasi D, Arnold J, Van Liew M, Bingner R, Harmel R, Veith T (2007) Model evaluation guidelines for systematic quantification of accuracy in watershed simulations. *Trans Am Soc Agric Biol Eng* 50(3):885–900. <https://doi.org/10.13031/2013.23153>.
- Moss R, Babiker M, Brinkman S, Calvo E, Carter T, Edmonds J, et al (2008) Towards New Scenarios for Analysis of Emissions, Climate Change, Impacts and Response Strategies. Technical Summary. Intergovernmental Panel on Climate Change, Geneva, 25
- Mu Q, Zhao M, Running SW (2011) Improvements to a MODIS global terrestrial evapotranspiration algorithm. *Remote Sens Environ* 115(8):1781–1800. <https://doi.org/10.1016/j.rse.2011.02.019>
- Neitsch S, Arnold J, Kiniry J, Williams J (2000). Soil and Water Assessment Tool Theoretical Documentation (2000) Grassland, Soil and Water Research Laboratory, Agricultural Research Service. Texas 76502:506
- Nerantzaki SD, Efstathiou D, Giannakis GV, Kritsotakis M, Grillakis MG, Koutroulis AG, Tsanis IK, Nikolaidis NP (2019) Climate change impact on the hydrological budget of a large Mediterranean island. *Hydrolog Sci J* 64(10):1190–1203. <https://doi.org/10.1080/02626667.2019.1630741>
- Nyeko M (2014) Hydrologic Modelling of Data Scarce Basin with SWAT Model: Capabilities and Limitations. *Water Resour Manag* 29(1):81–94. <https://doi.org/10.1007/s11269-014-0828-3>
- Odusanya AE, Mehdi B, Schurz C et al (2019) Multi-site calibration and validation of SWAT with satellite-based evapotranspiration in a data-sparse catchment in southwestern Nigeria. *Hydrol Earth Syst Sci* 23:1113–1144. <https://doi.org/10.5194/hess-23-1113-2019>
- Parajuli PB, Jayakody P, Ouyang Y (2018) Evaluation of Using Remote Sensing Evapotranspiration Data in SWAT. *Water Resour Manage* 32:985–996. <https://doi.org/10.1007/s11269-017-1850-z>
- Patrikaki O (2010). Hydrogeological Conditions of Potamia Drainage Basin in North Greece. Department of Geology, Aristotle University of Thessaloniki. (Ph.D. thesis, in Greek with English summary)
- Patrikaki O., Kazakis N., Voudouris K. (2012). Vulnerability map: A useful tool for groundwater protection: An example from Mouriki basin, North Greece, *Fresenius Environmental Bulletin*, Vol. 21 No 8c, p 2516- 2521.
- Running S, Mu Q, Zhao M, Moreno A (2019) MOD16A2GF MODIS/Terra Net Evapotranspiration Gap-Filled 8-Day L4 Global 500 m SIN Grid V006. NASA EOSDIS Land Processes DAAC. <https://doi.org/10.5067/MODIS/MOD16A2GF.006>
- Sutanudjaja EH, van Beek R, Wanders N, Wada Y et al (2018) PCR-GLOBWB 2: a 5 arcmin global hydrological and water resources model. *Geosci Model Develop* 11(6):2429–2453. <https://doi.org/10.5194/gmd-11-2429-2018>
- Scanlon BR, Healy RW, Cook PG (2002) Choosing appropriate techniques for quantifying groundwater recharge. *Hydrogeol J* 10:18–39
- Taylor R, Scanlon B, Doll P et al (2013) Ground water and climate change. *Nature Clim Change* 3:322–329. <https://doi.org/10.1038/nclimate1744>
- Tuo Y, Duan Z, Disse M, Chiogna G (2016) Evaluation of precipitation input for SWAT modeling in alpine catchment: A case study in the Adige river basin (Italy). *Sci Tot Environ* 573:66–82. <https://doi.org/10.1016/j.scitotenv.2016.08.034>
- Van Loon A, Rangelcroft S, Coxon G, Naranjo JAB et al (2019) Using paired catchments to quantify the human influence on hydrological droughts. *Hydrol Earth Syst Sci* 23(3):1725–1739. <https://doi.org/10.5194/hess-23-1725-2019>
- Venetsanou P, Anagnostopoulou C, Loukas A, Voudouris K (2020) Hydrological impacts of climate change on a data-scarce Greek catchment. *Theor Appl Climatol* 140:1017–1030. <https://doi.org/10.1007/s00704-020-03130-6>
- Zhang H, Wang B, Li Liu D, Zhang M, Leslie LM, Yu Q (2020) Using an improved SWAT model to simulate hydrological responses to land use change: a case study of a catchment in tropical Australia. *J Hydrol* 124822. <https://doi.org/10.1016/j.jhydrol.2020.124822>